Construction of a 100-TW laser and its applications in EUV laser, wakefield accelerator, and nonlinear optics

Jyhpyng Wang (汪治平)

Institute of Atomic and Molecular Sciences
Academia Sinica, Taiwan

National Central University, Taiwan

National Taiwan University, Taiwan

Collaborators

Core members of the 10-TW and 100-TW laser facilities

Prof. Prof. Szu-yuan Chen (陳賜原), Academia Sinica, Taiwan
Prof. Jiunn-Yuan Lin (林俊元), National Chung-Cheng Univ., Taiwan
Prof. Hsu-Hsin Chu (朱旭新), National Central Univ., Taiwan

Theoretical analysis

Prof. Gin-yih Tsaur (曹景懿), Tunghai Univ., Taiwan

Computer simulation

Prof. Shih-Hung Chen (陳仕宏), National Central Univ., Taiwan

Outline

- High-intensity lasers
- High-brightness EUV lasers
- Laser-wakefield electron accelerators
- Relativistic plasma nonlinear optics

High-intensity lasers

- Generation of femtosecond laser pulses
- Amplification of femtosecond laser pulses
- Measurement of femtosecond optical waveforms
- Synthesis of femtosecond optical waveforms
- High-intensity lasers in Taiwan

Pulse compression by self-focusing

optical Kerr effect: $n = n_0 + n_2 I$

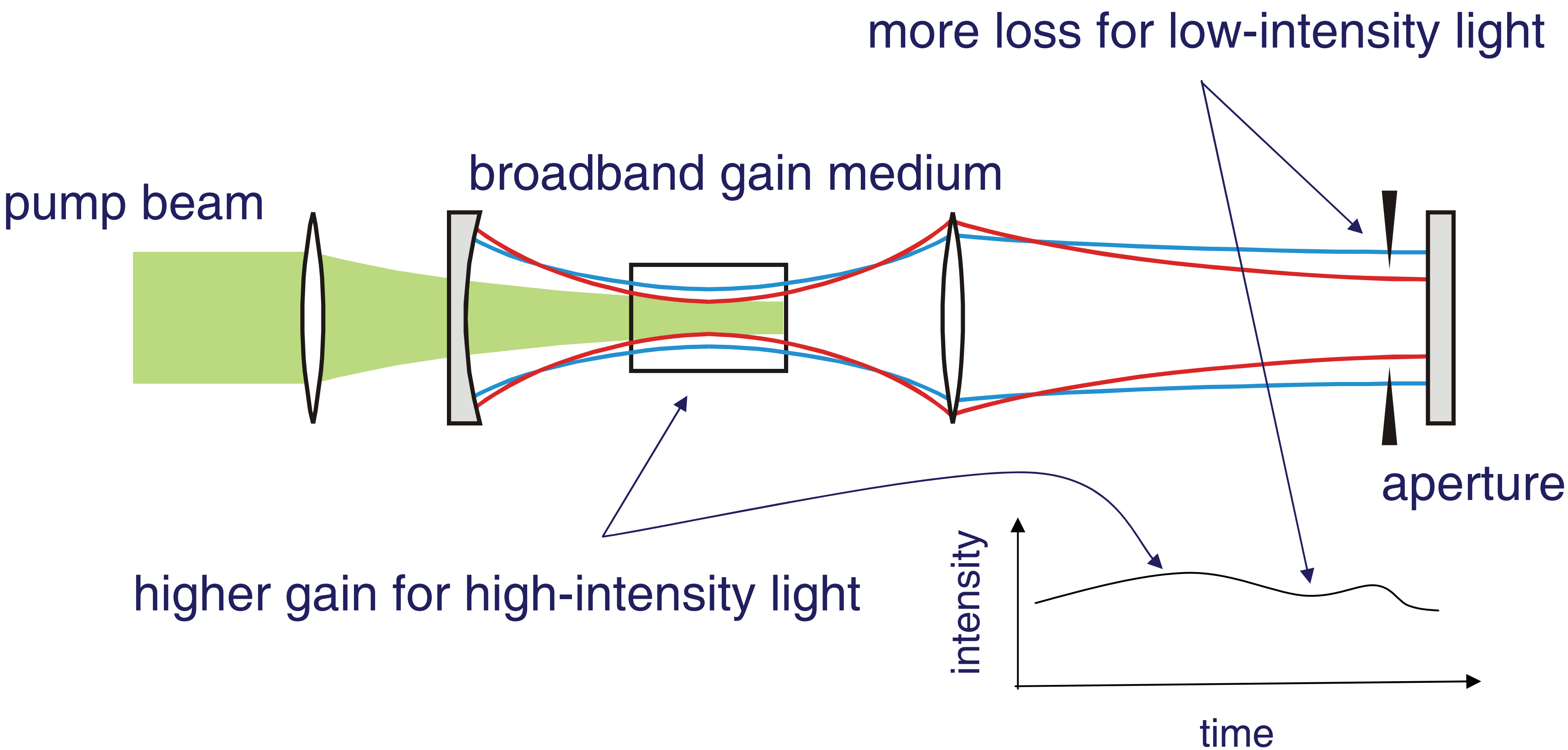

Capitalism for laser

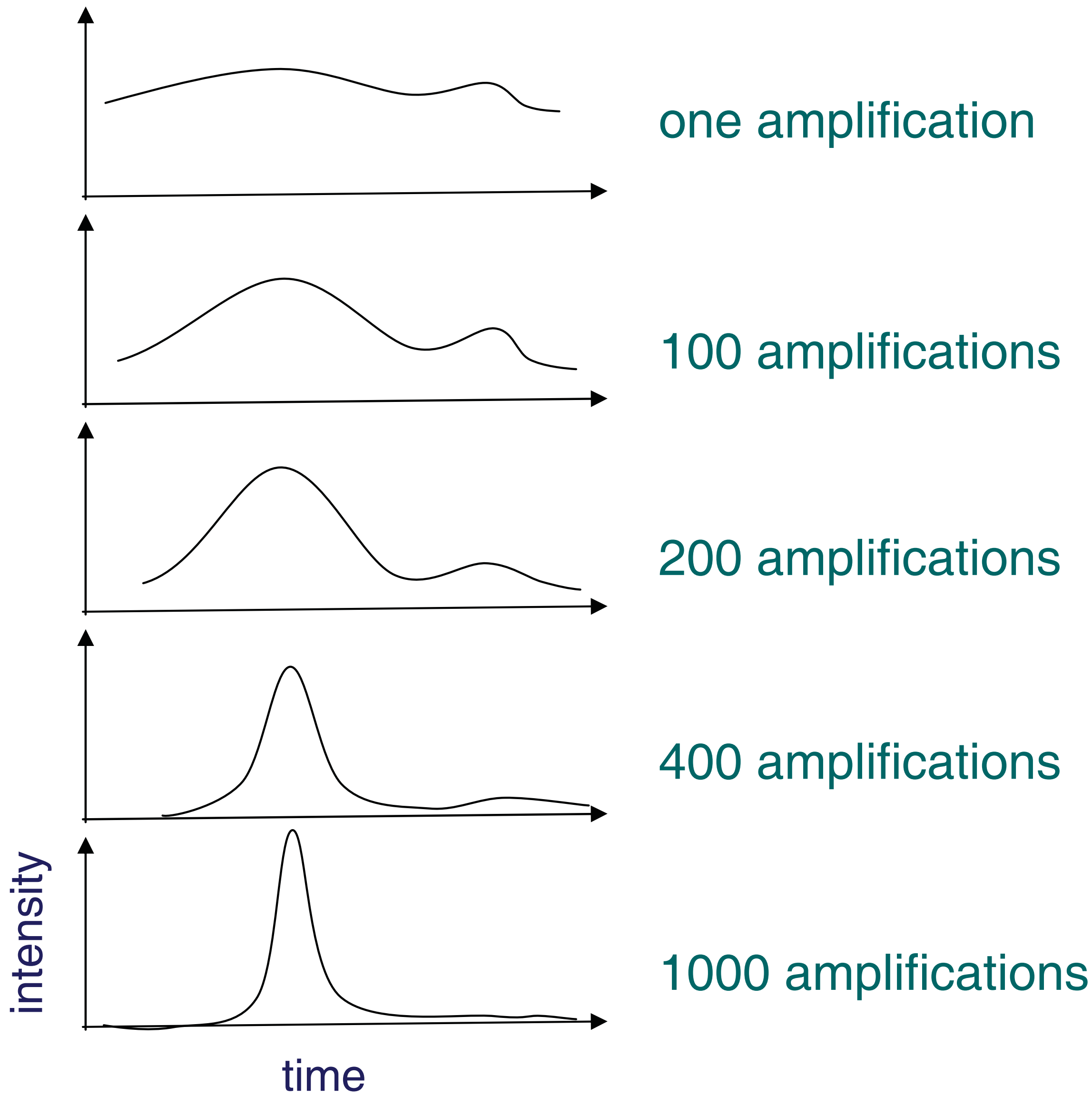

Compensation for dispersion

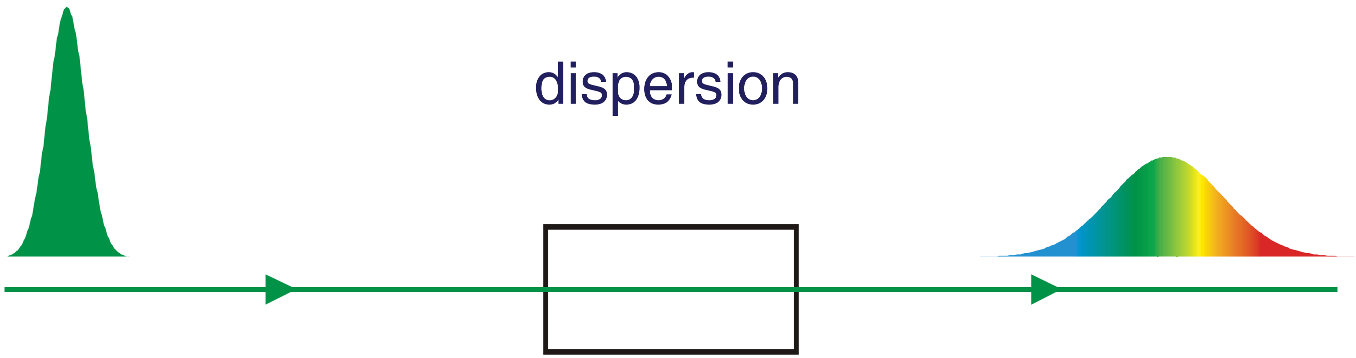

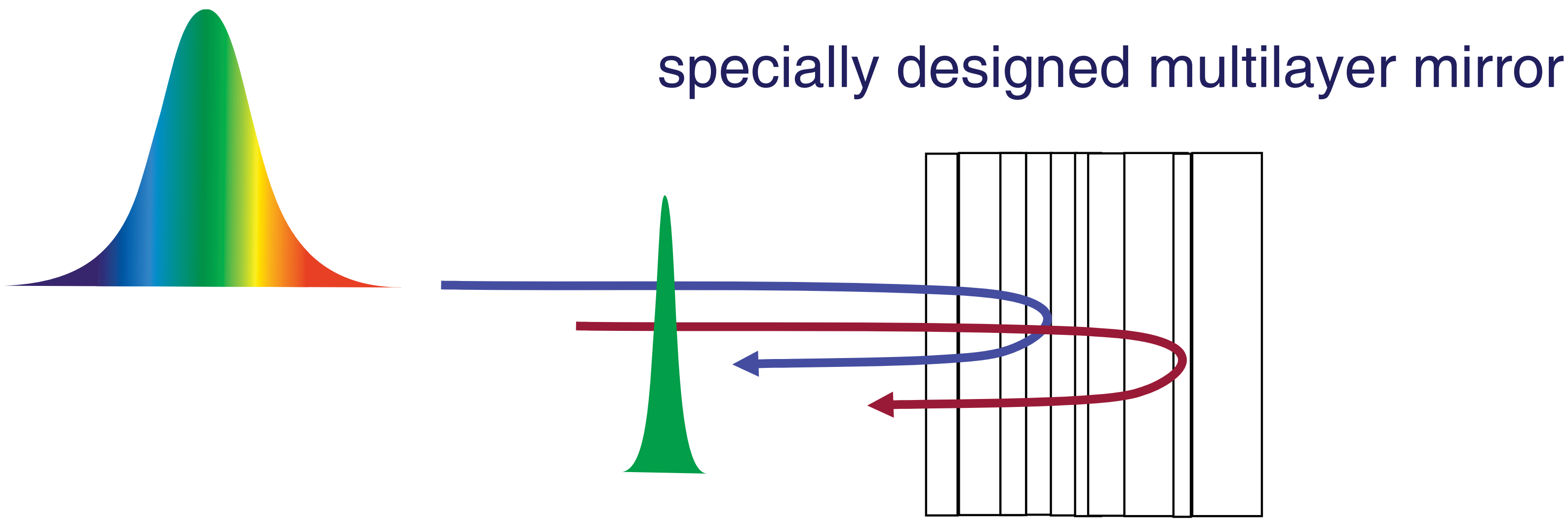

Chirped pulse amplification

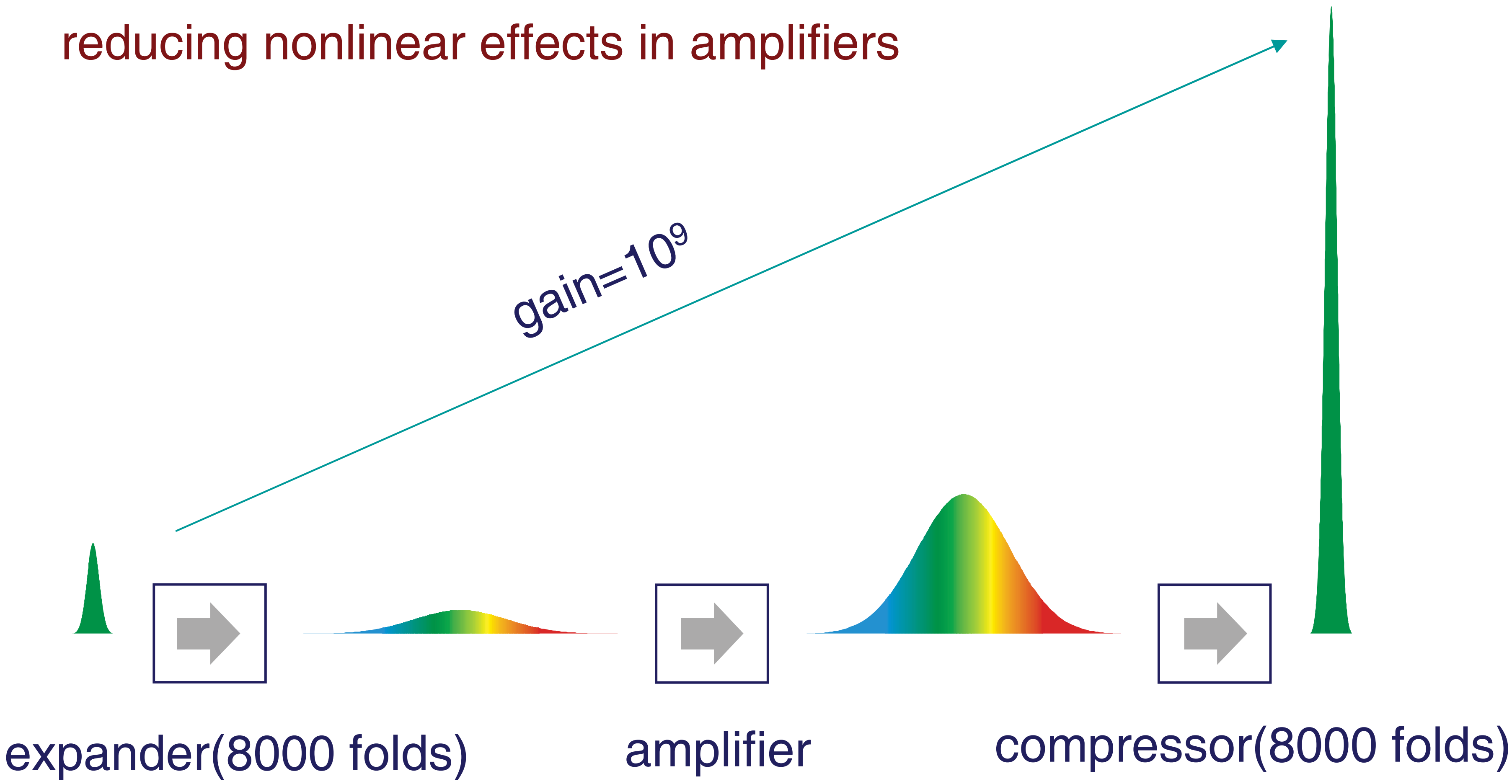

Principle of pulse stretcher

Shorter wavelength has longer optical path,
the difference is comparable to grating size.

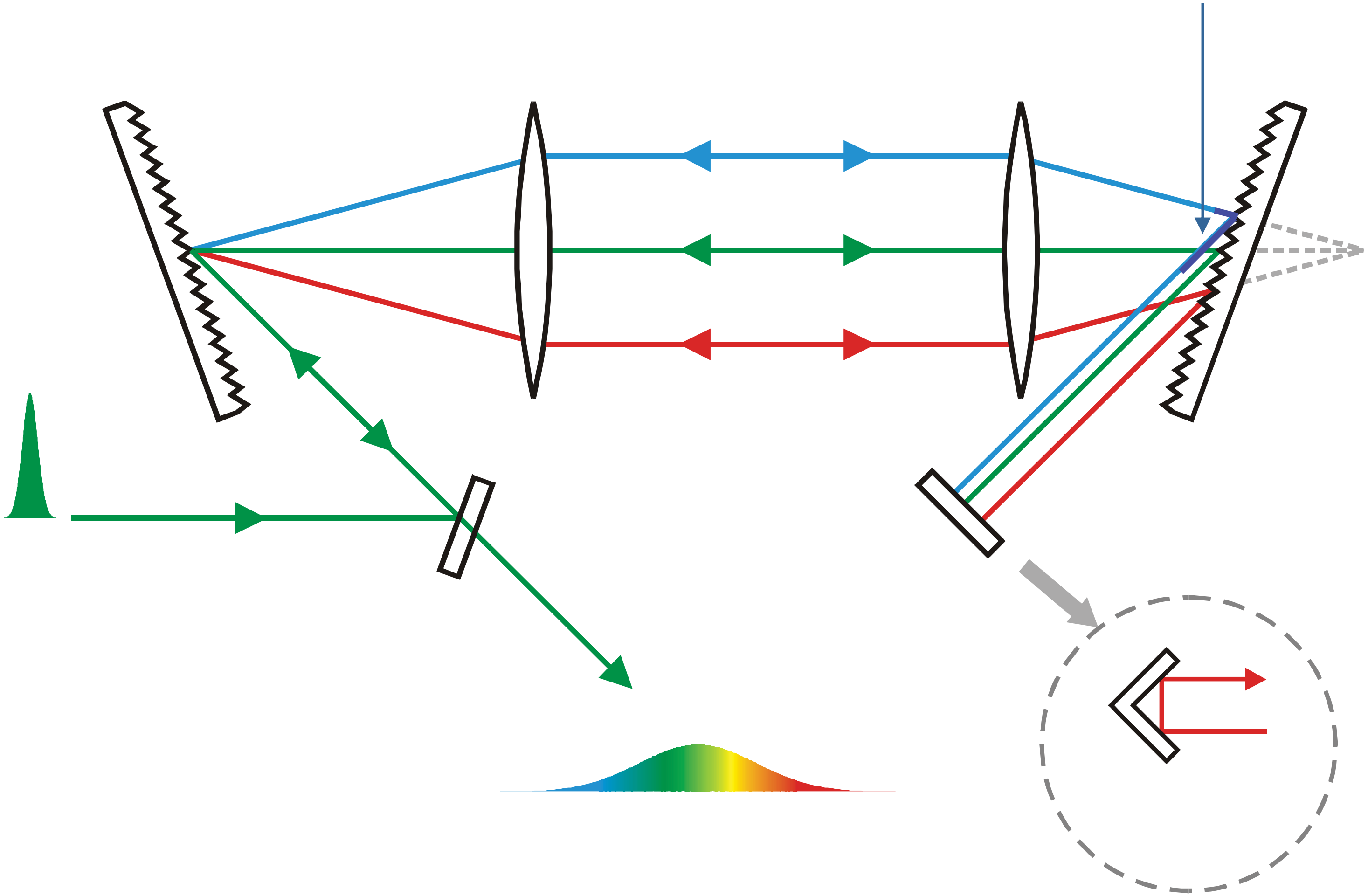

Principle of pulse compressor

Longer wavelength has longer optical path, the difference is comparable to grating size.

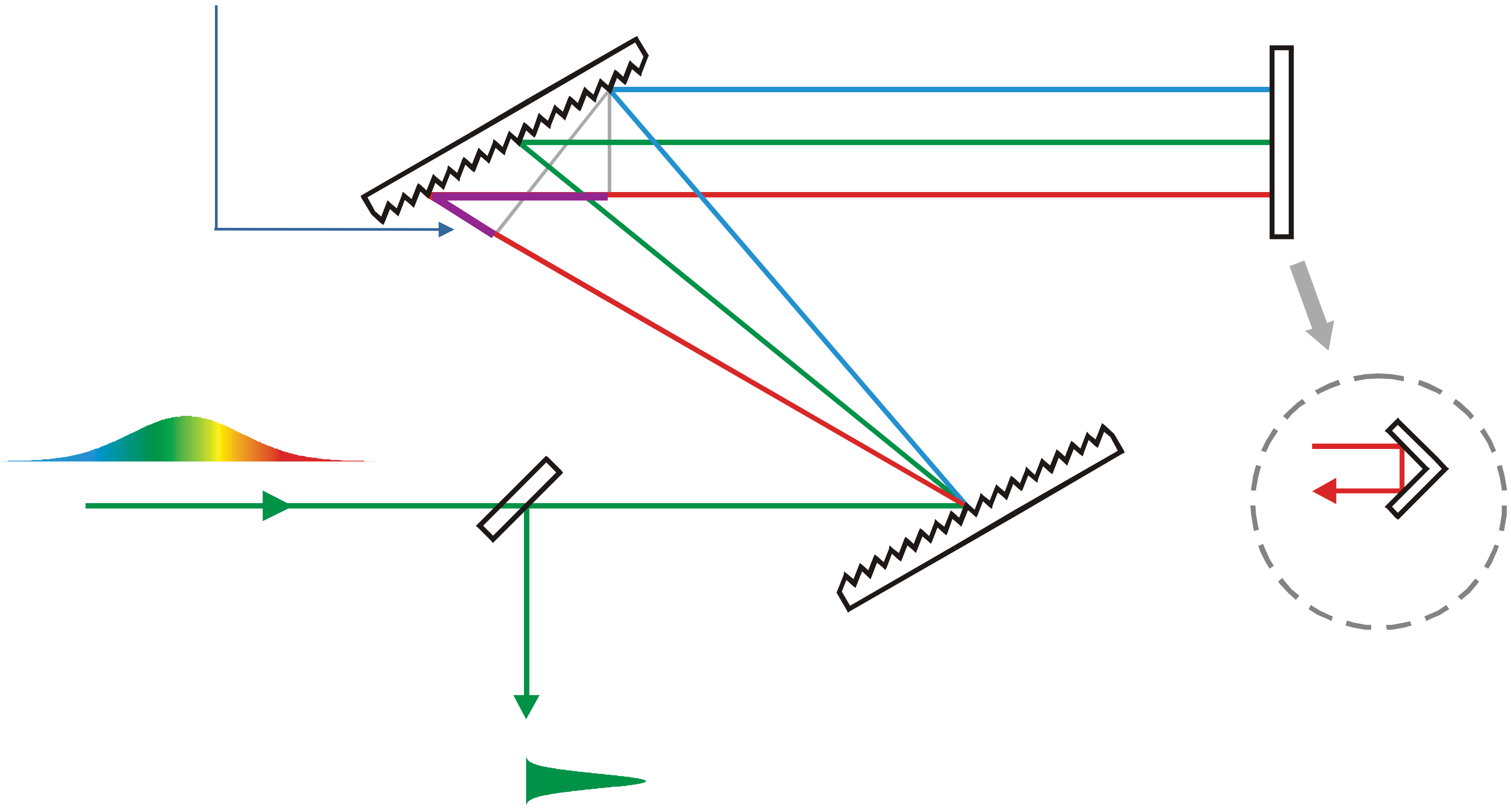

10-TW laser at IAMS, Academia Sinica

25-fs oscillator

pulse stretcher

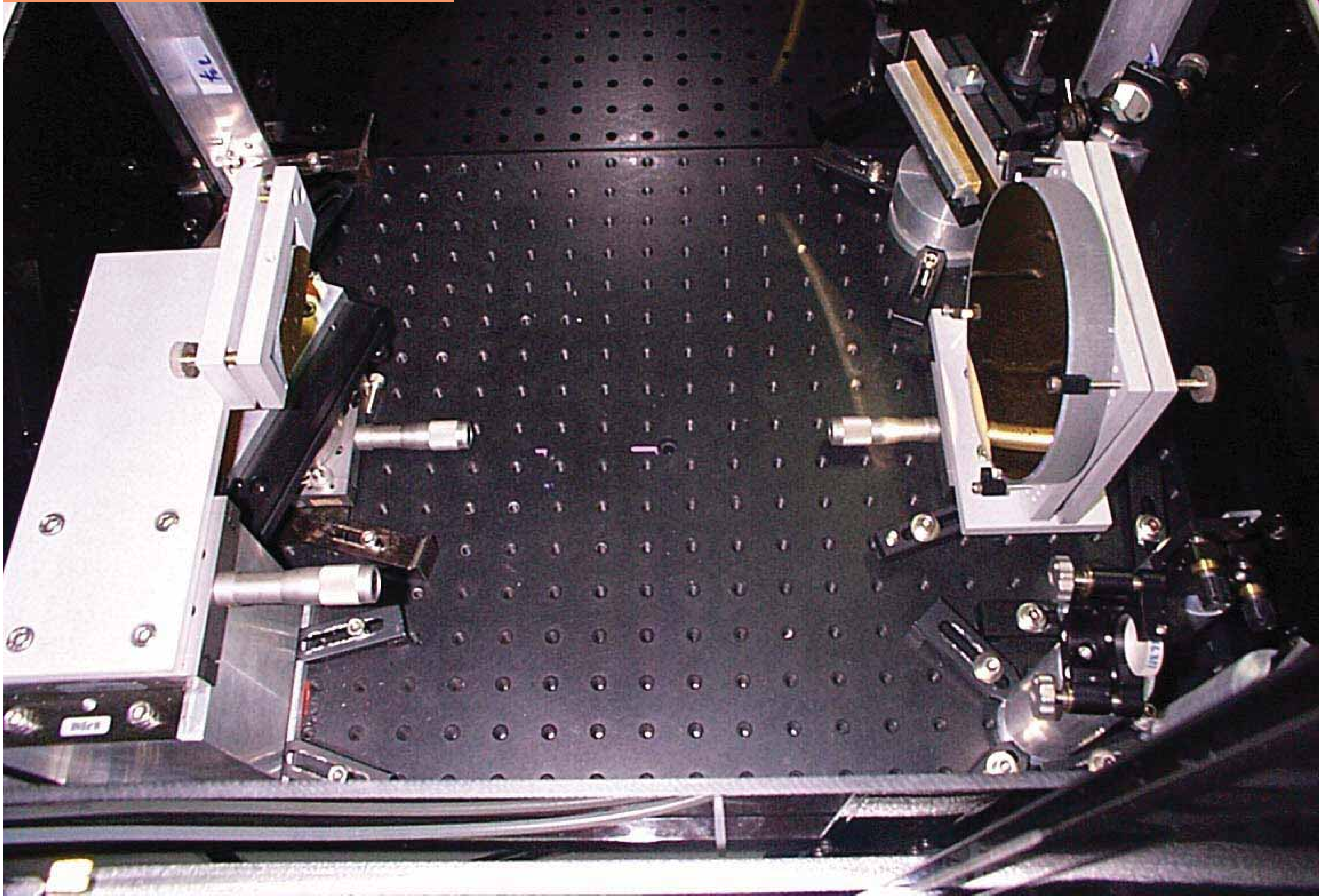

preamplifier

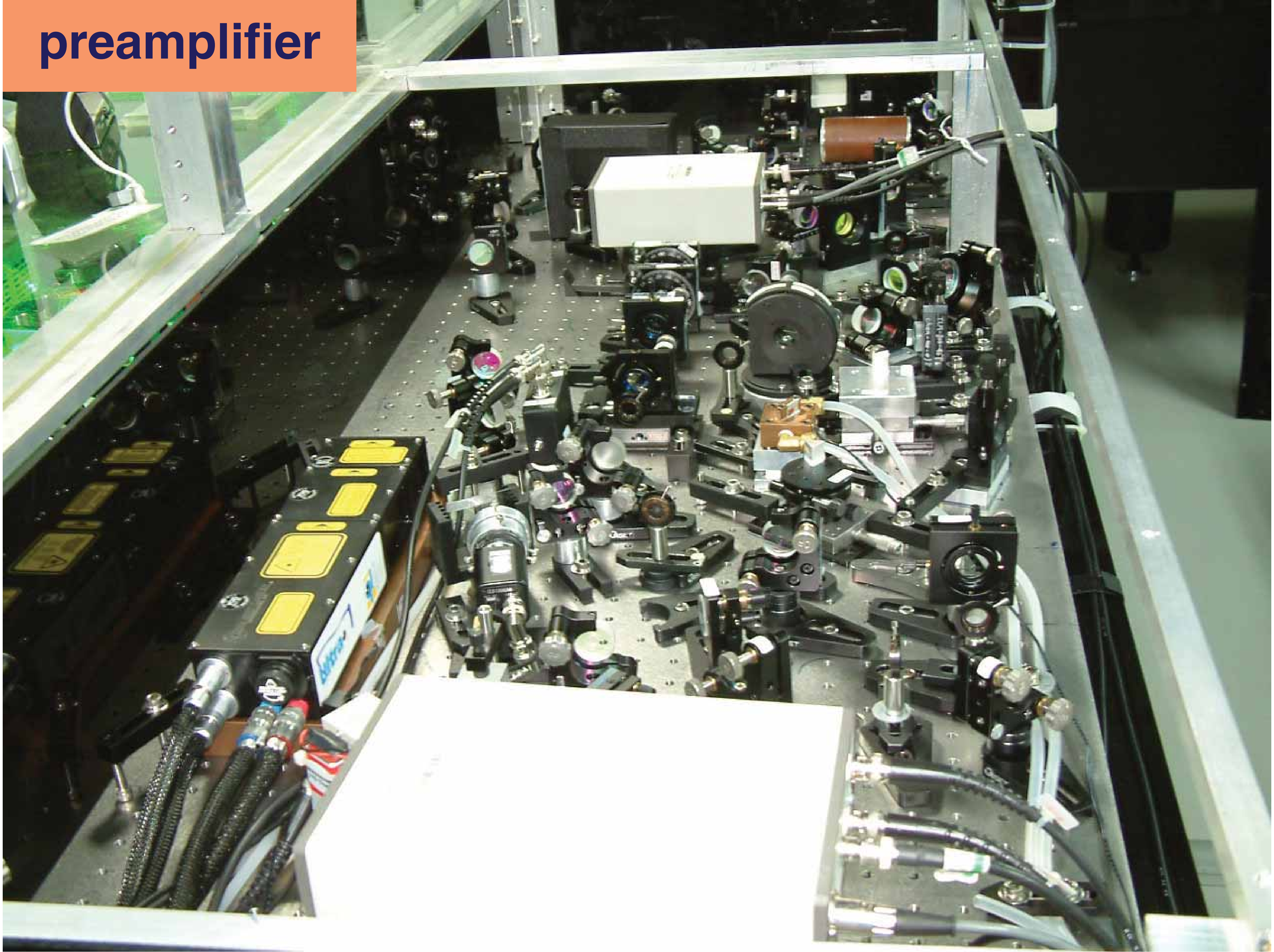

second-stage amplifier

third-stage amplifier

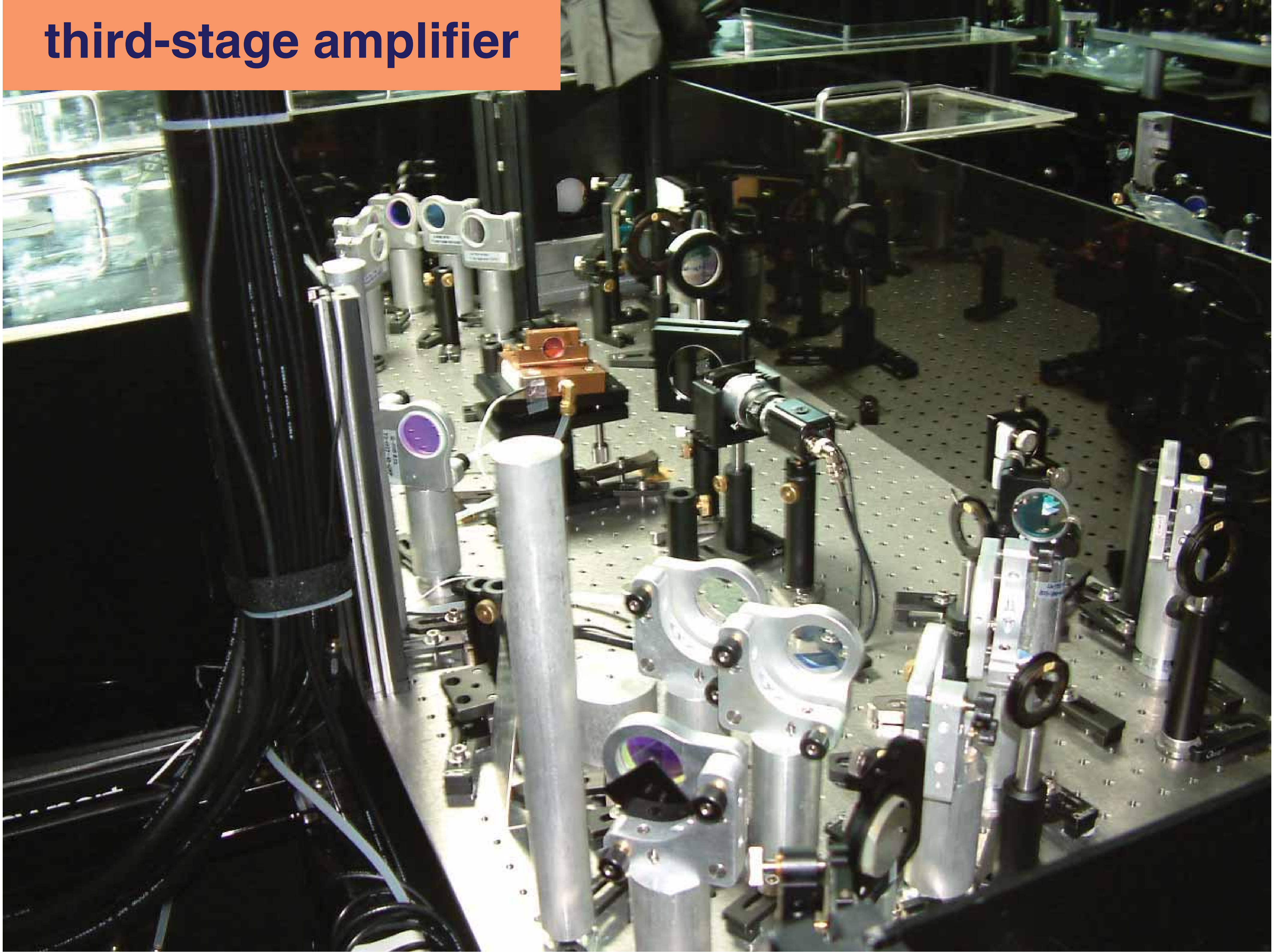

pulse compressor

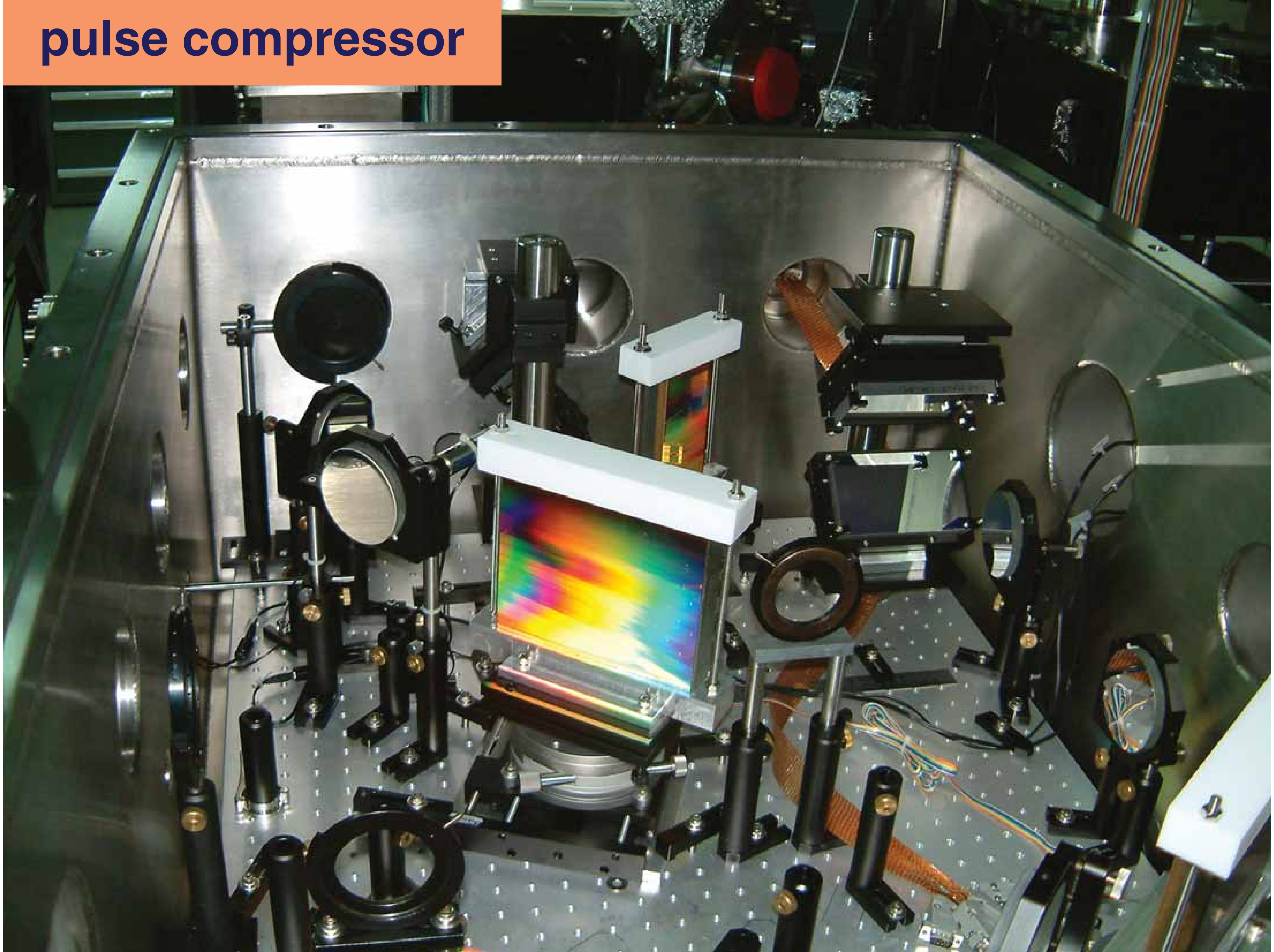

100-TW laser at Nat'l Central Univ.

preamplifier

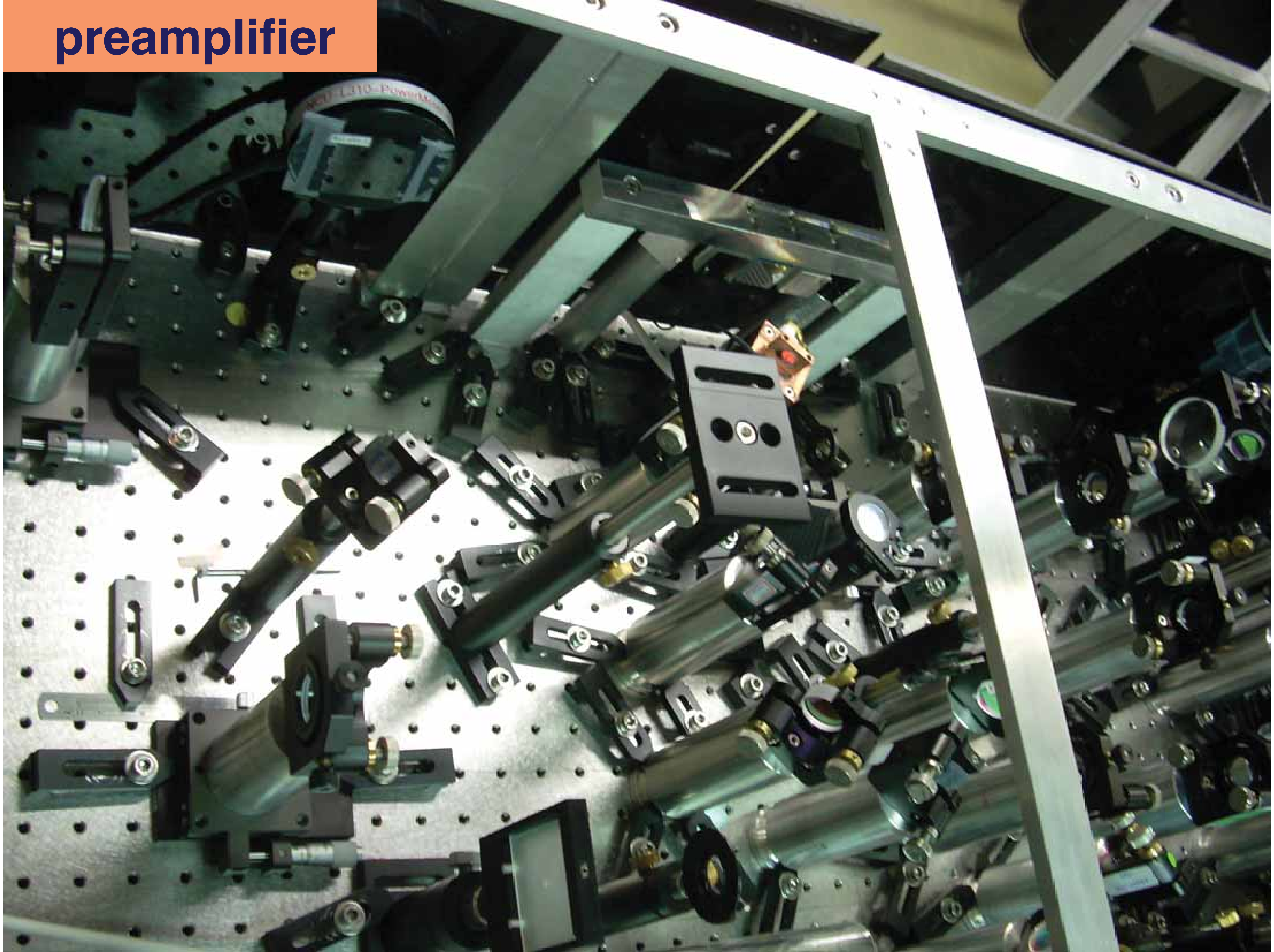

pulse stretcher

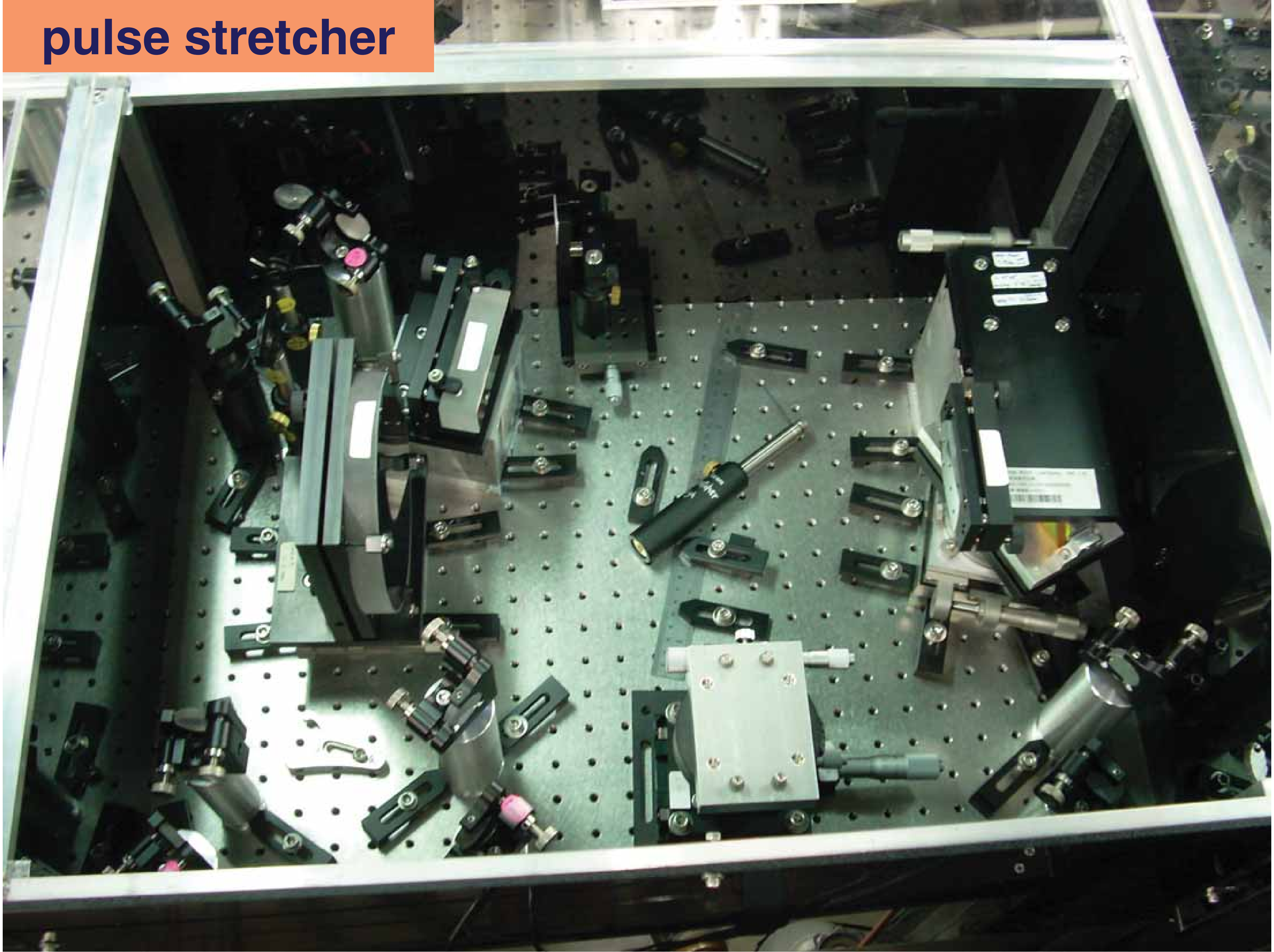

second-stage amplifier

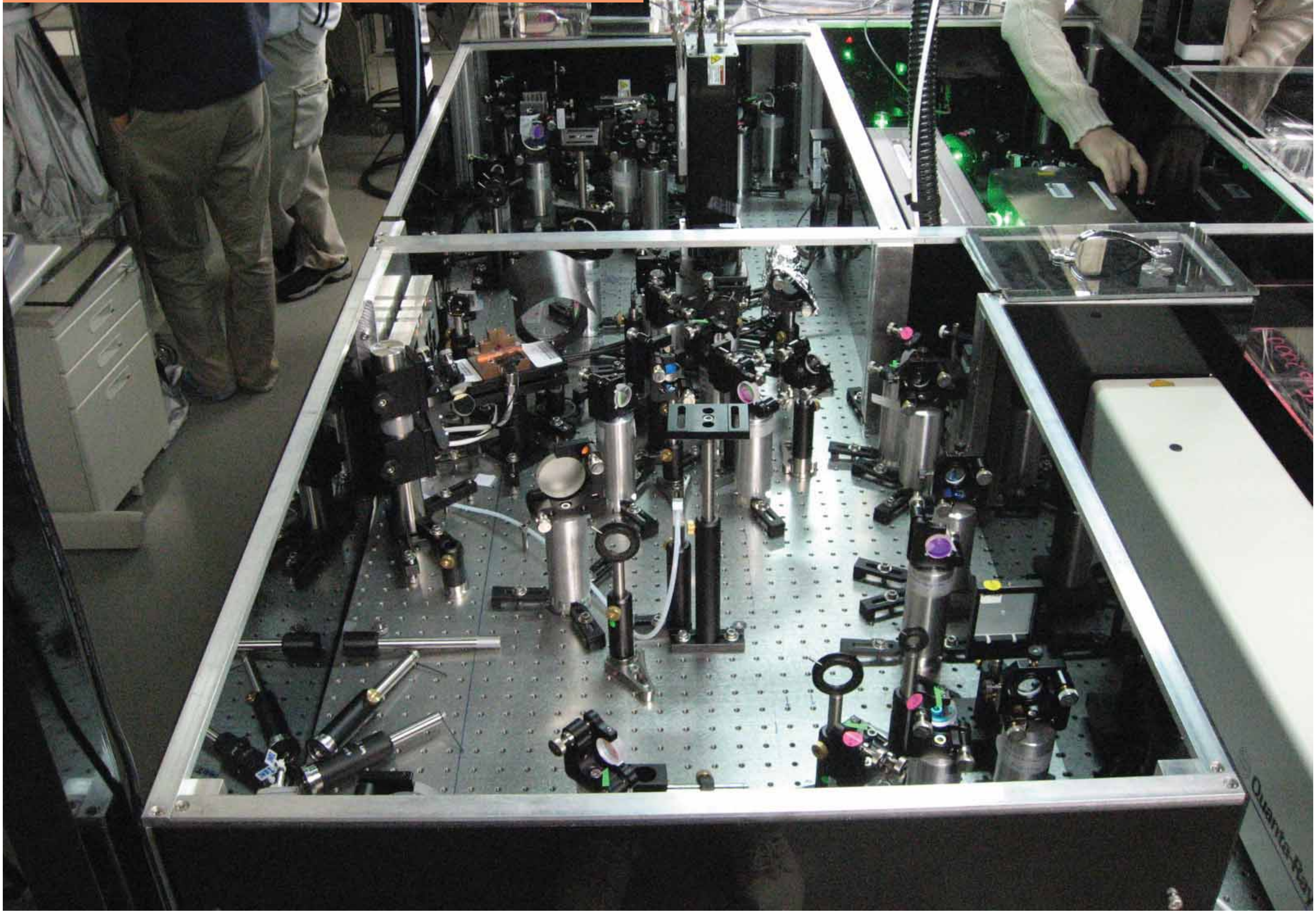

third-stage amplifier

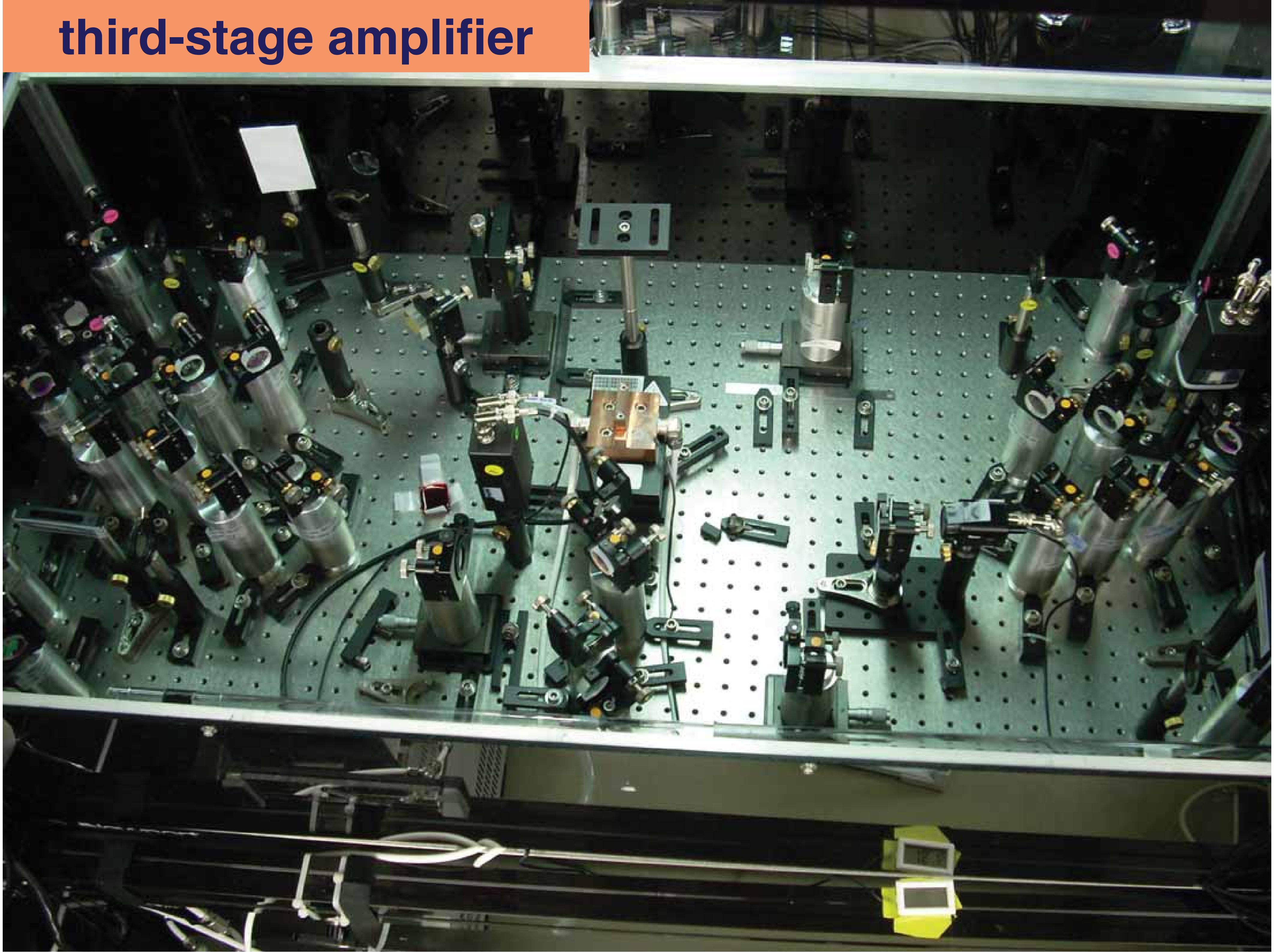

100-TW final stage amplifier

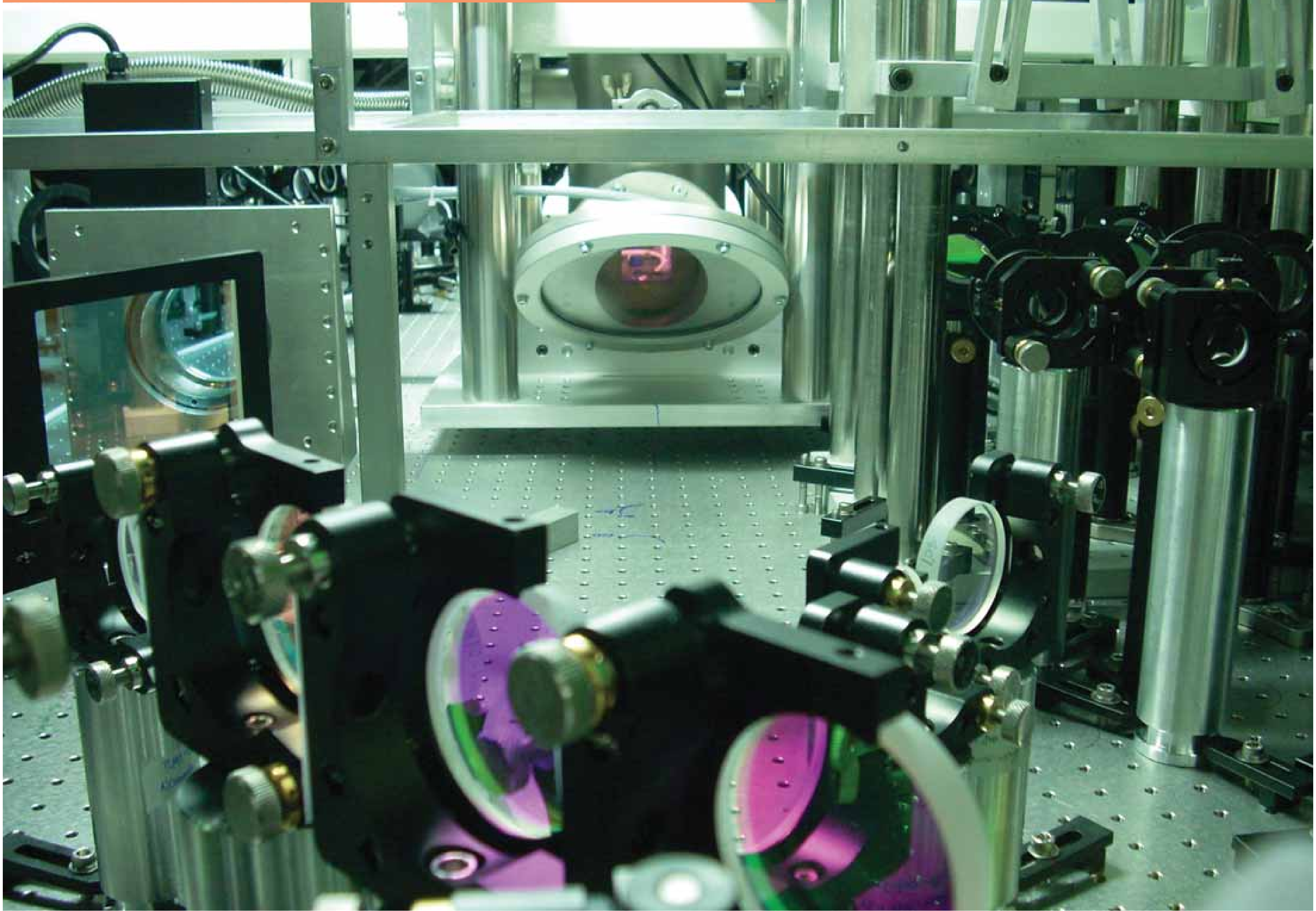

view of the laser from a corner

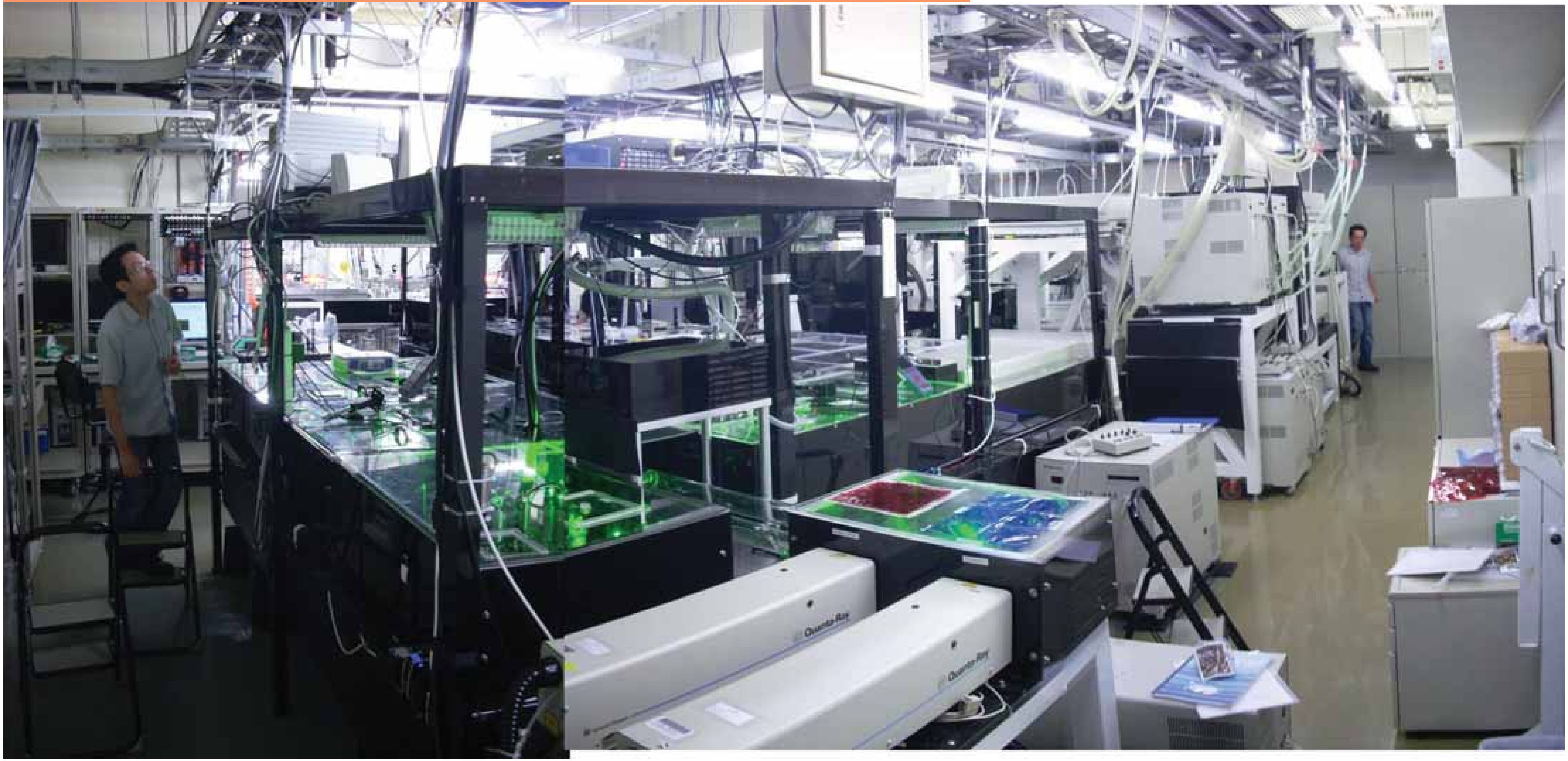

16 Nd:YAG pump lasers

compressor array

beam switching chambers

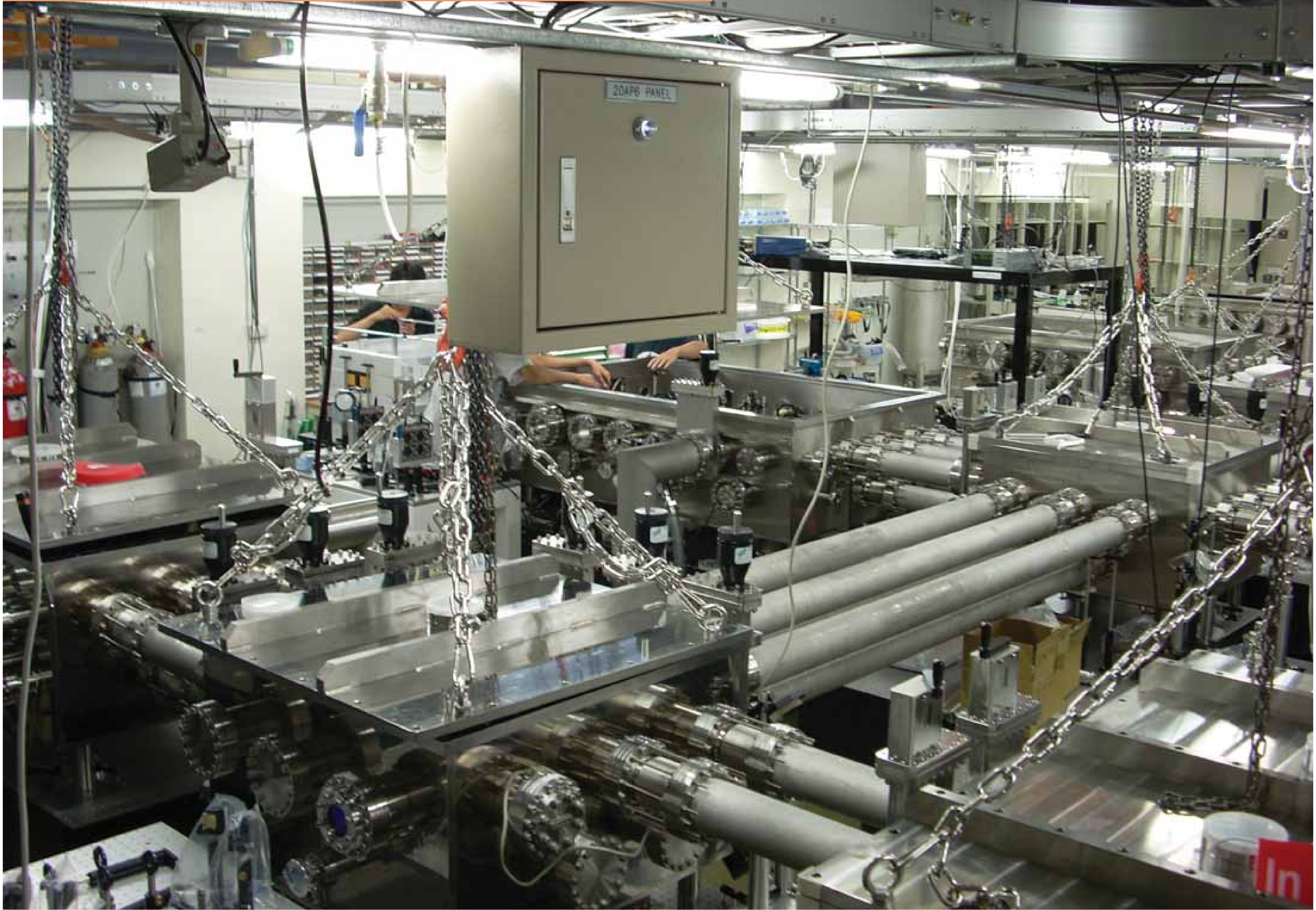

experimental station

experimental stations

full view of the laboratory

100-TW laser after focusing

- peak power: 3J/30 fs $=10^{14}$ W (10,000 nuclear power plants)
- peak intensity: 10^{20} W/cm^2 (sunshine at noon = 0.1 W/cm^2)
- electric field: 3.2×10^{13} V/m (50× Coulomb field in hydrogen)
- optical pressure: 2.2×10^{10} atm (center of the Sun)
- plasma temperature: 10^7 K (center of the Sun)
- acceleration on electron: 5×10^{23} g (near a black hole)

The problem of limited interaction length

diffraction

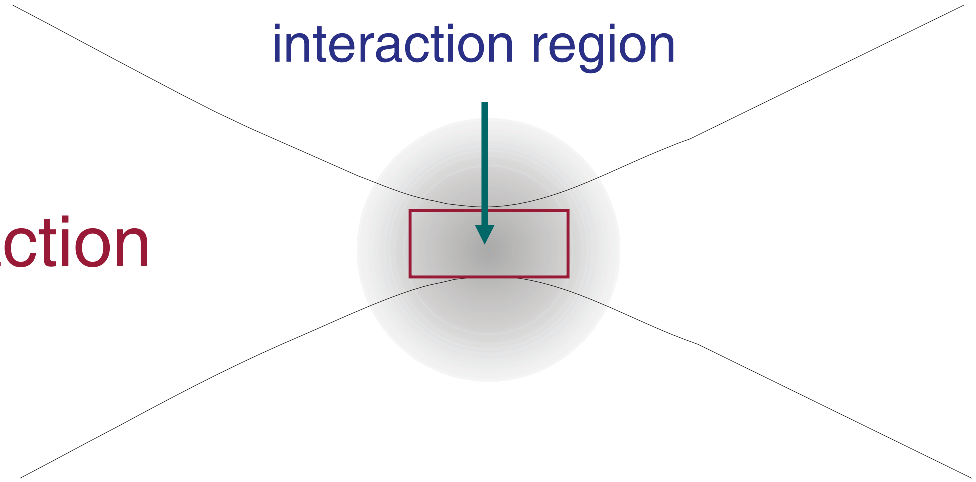

tighter focus → shorter interaction length

ionization defocusing

high index of refraction

laser pulse

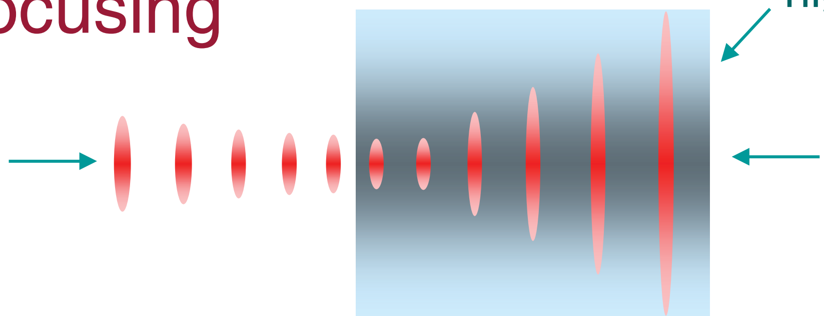

low index of refraction

defocusing reduces the intensity

Plasma-waveguide formation from a line focus

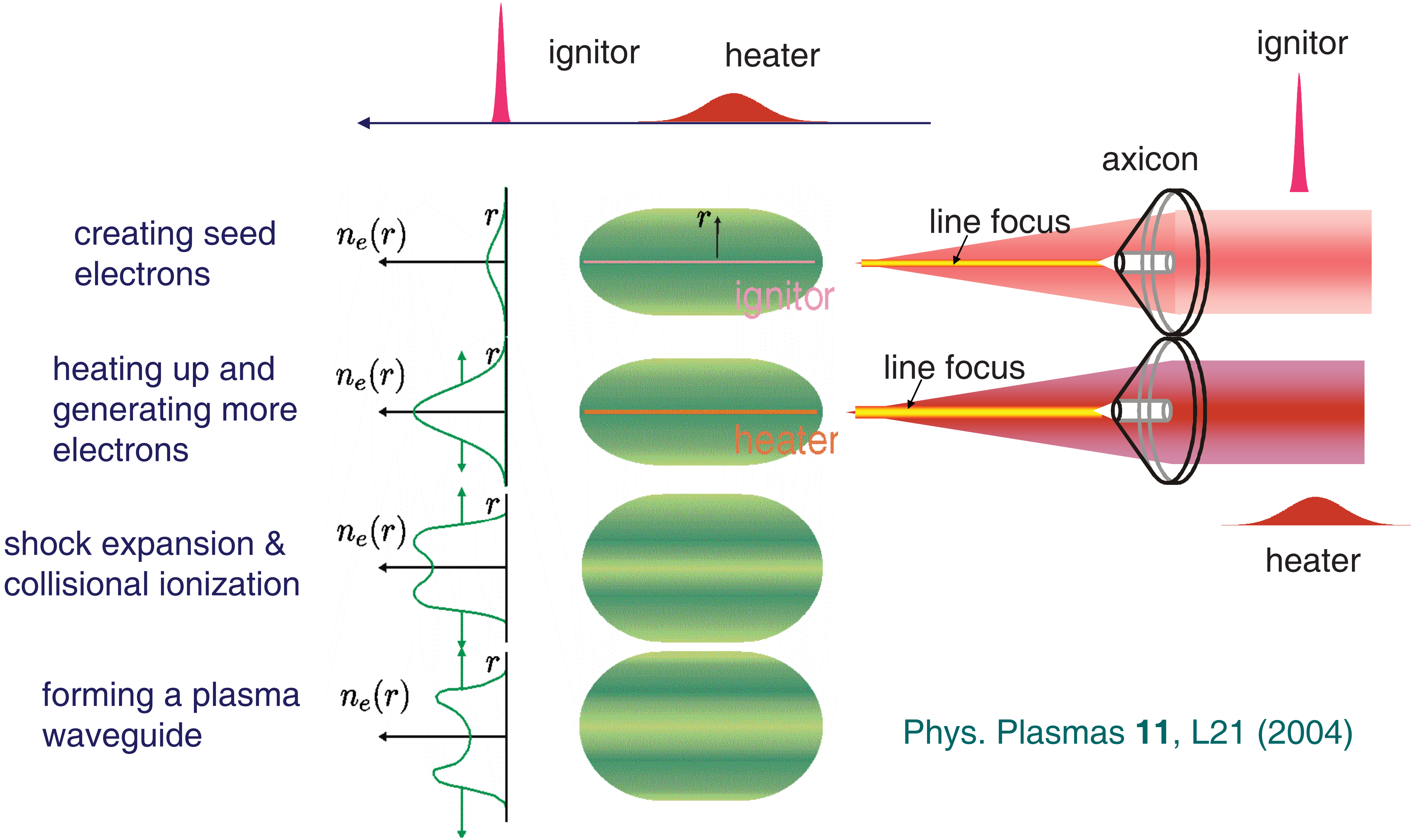

Phys. Plasmas **11**, L21 (2004)

Laser drilled plasma waveguide

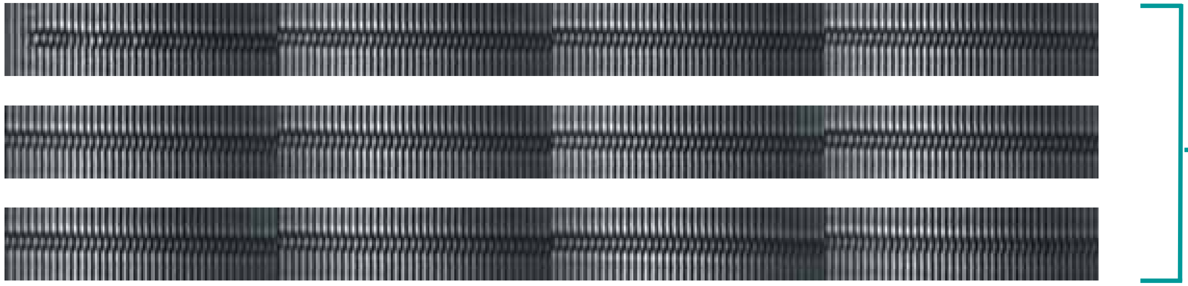

length > 1.2 cm

density variation < 20%

ignitor: 15 mJ, 55 fs

heater: 85 mJ, 80 ps (1.1 ns delay)

probe: 1.2 ns after heater

Phys. of Plasma **11,** L21 (2004)

electron density profile

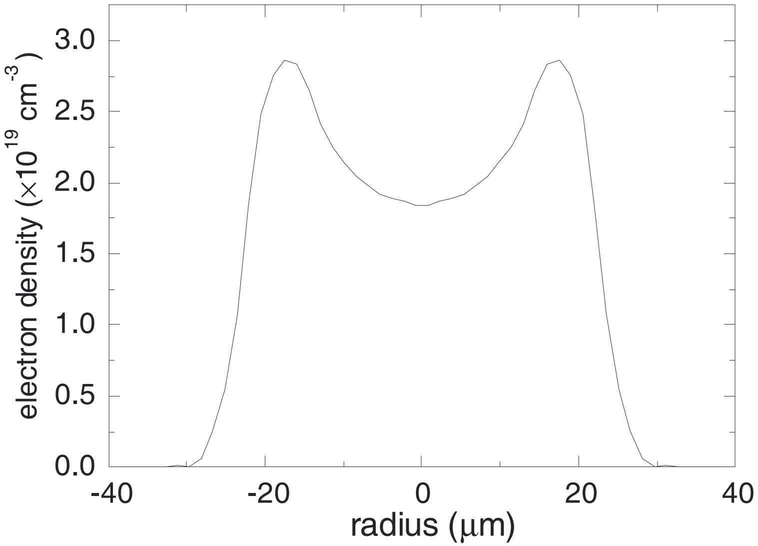

High-brightness EUV lasers

Phys. Rev. Lett. **99**, 063904 (2007)

Phys. Rev. A **76**, 053817 (2007)

Opt. Lett. **34**, 3562 (2009)

Energy levels of EUV lasers

He-Ne laser

Ne-like ions: Ar^{8+}, Ti^{12+}, Fe^{16+}

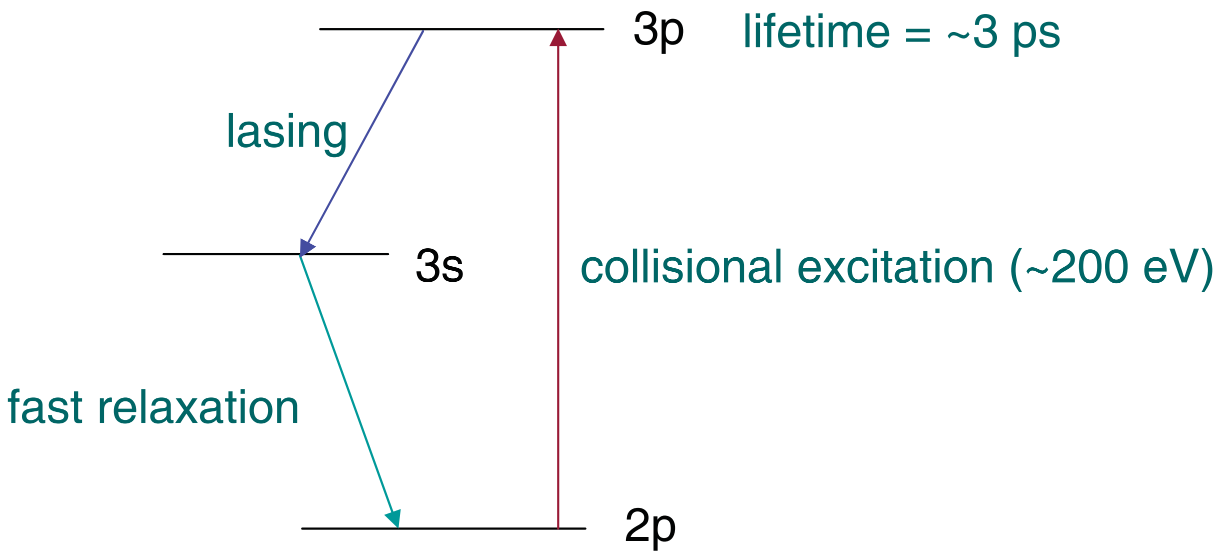

X-ray lasers powered by nuclear bomb for "Star Wars"

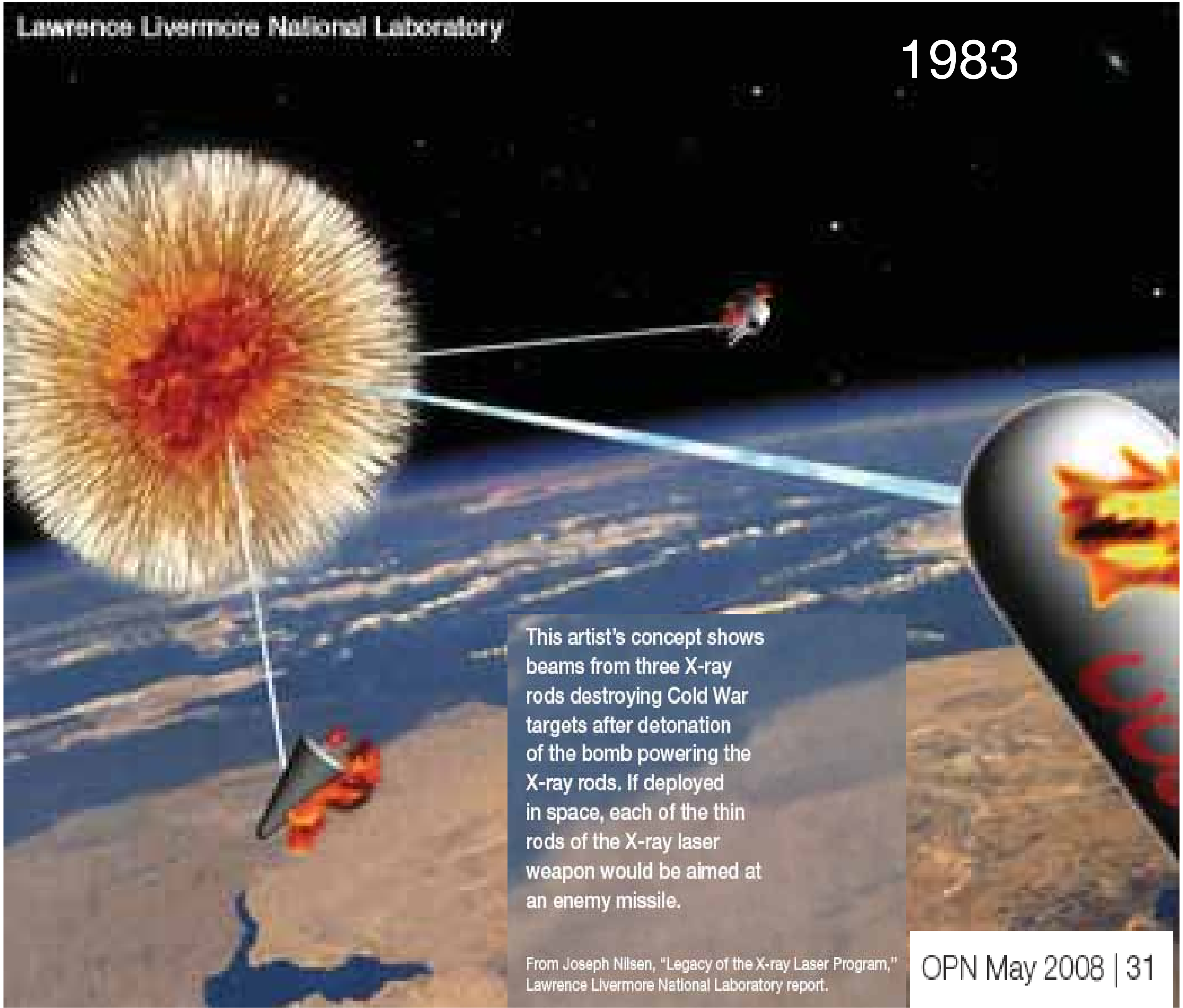

Optical-field ionization

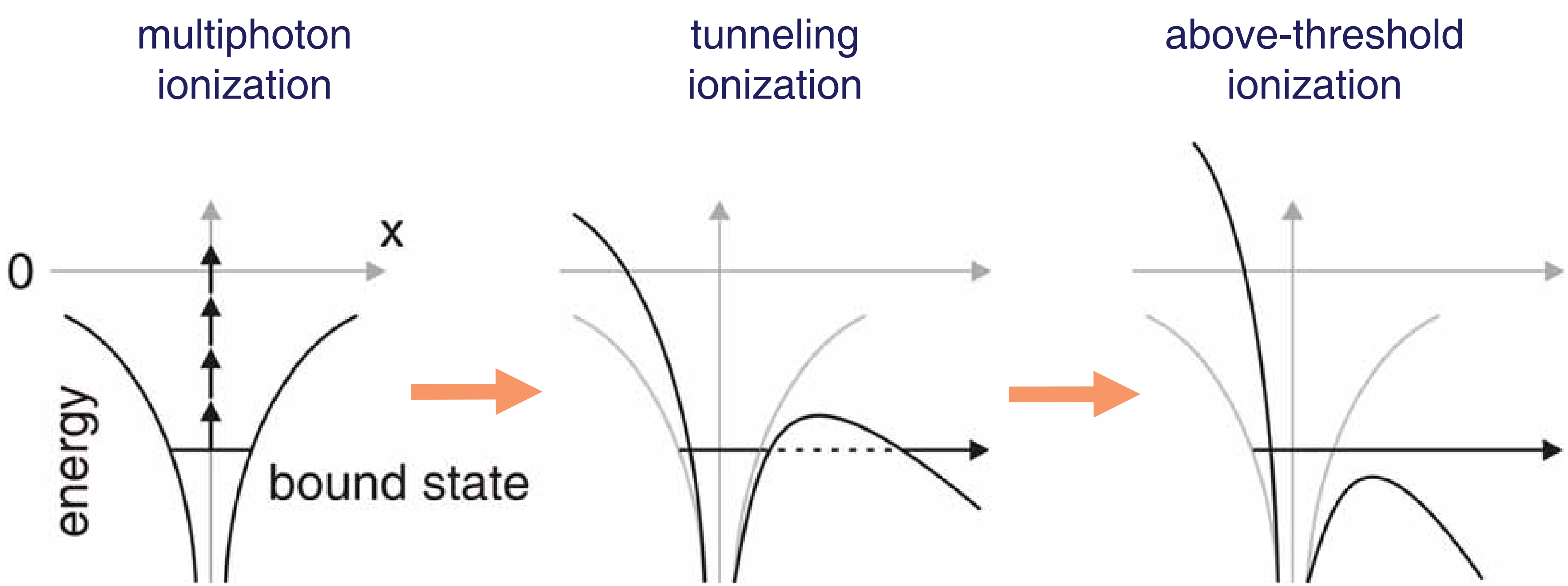

above-threshold
ionization heating

appearance intensity for 1^+ ion (λ=1 μm)

Xe: 8.7×10^{13} W/cm^2

He: 1.5×10^{15} W/cm^2

Ionization of Xe as a function of intensity

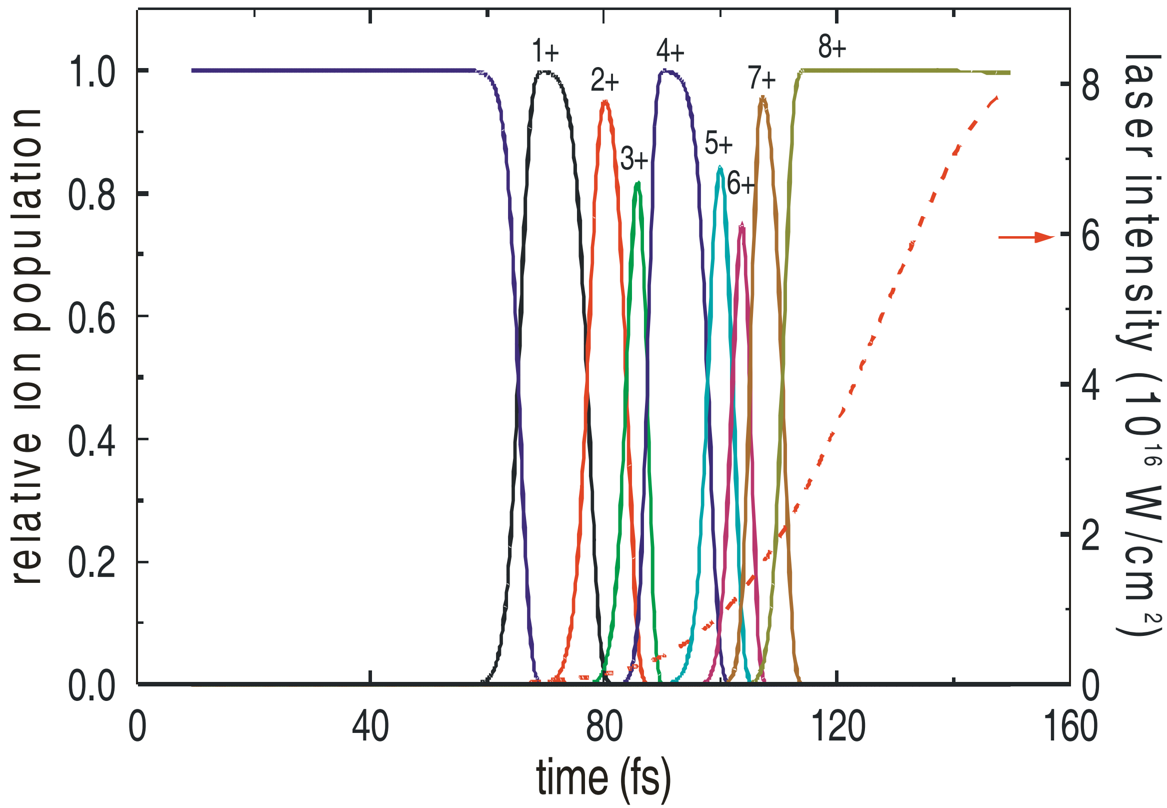

Ionization to a closed shell can be prepared by optical-field-ionization.

Energy levels of EUV lasers

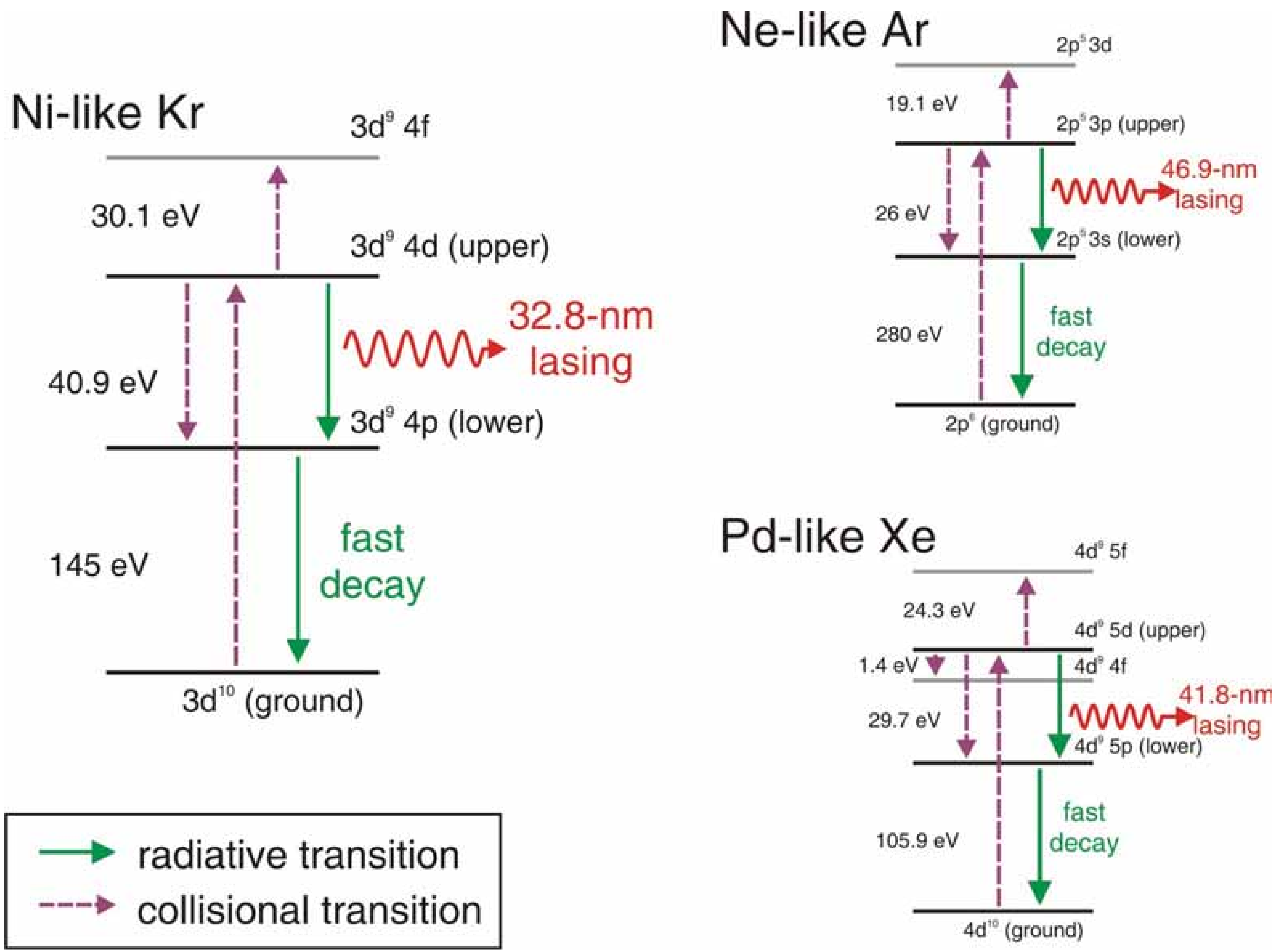

Pumping by optical-field ionization

ionization to specific ion stage → electrons gain energy → electron-ion collisional excitation → population inversion and lasing

↑

tunneling ionization

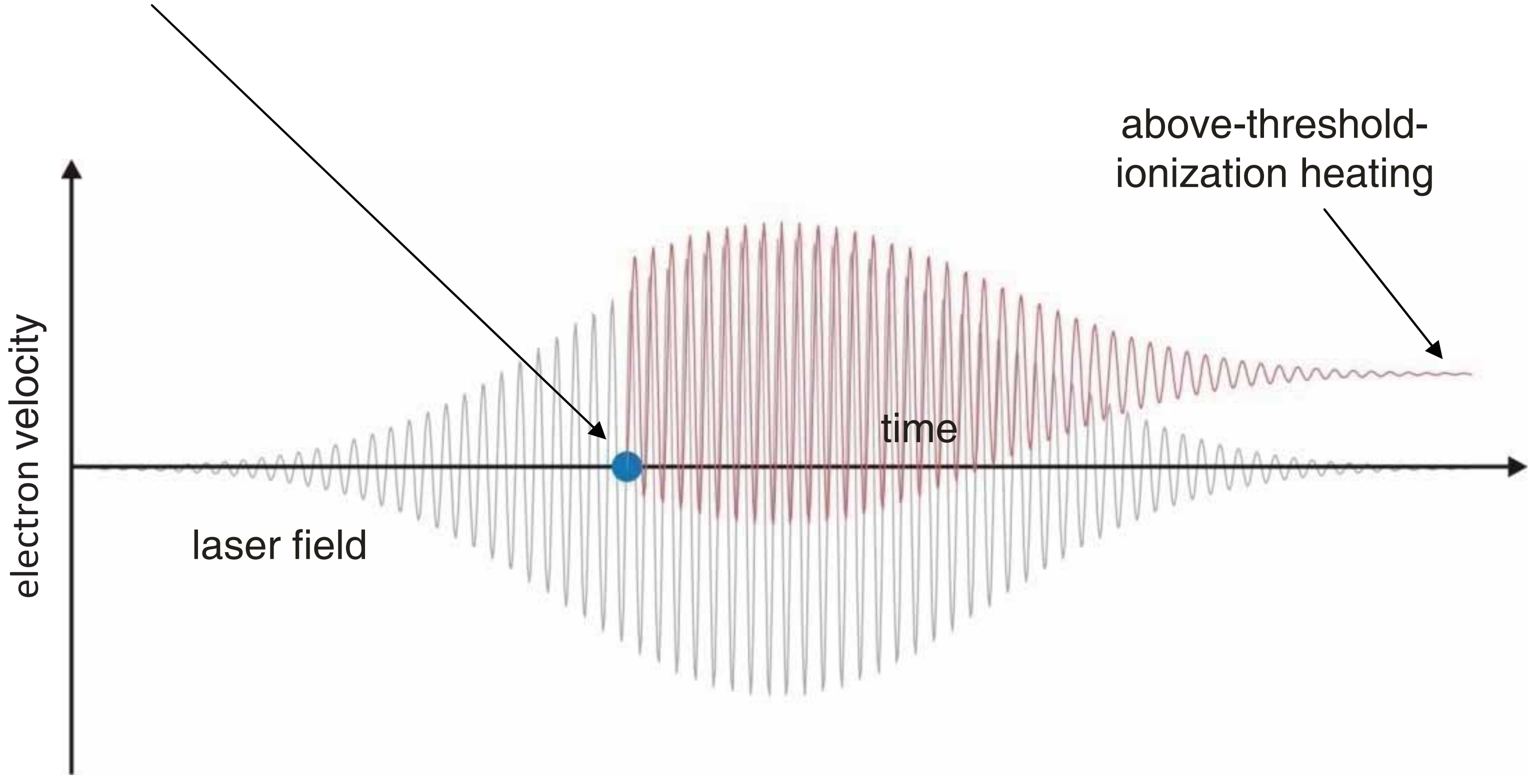

Gas-target EUV laser

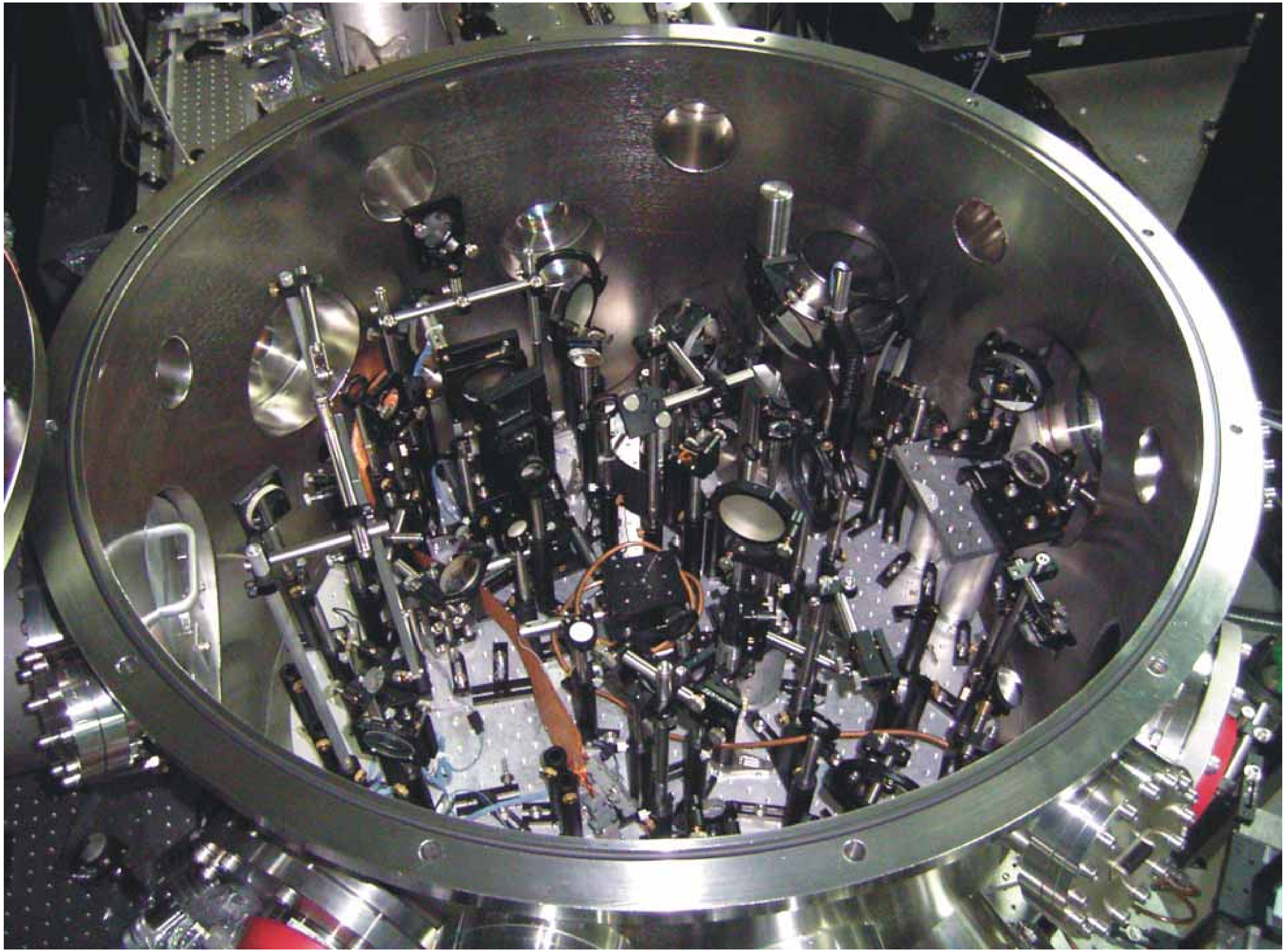

Longitudinally pumped optical-field-ionization EUV lasers

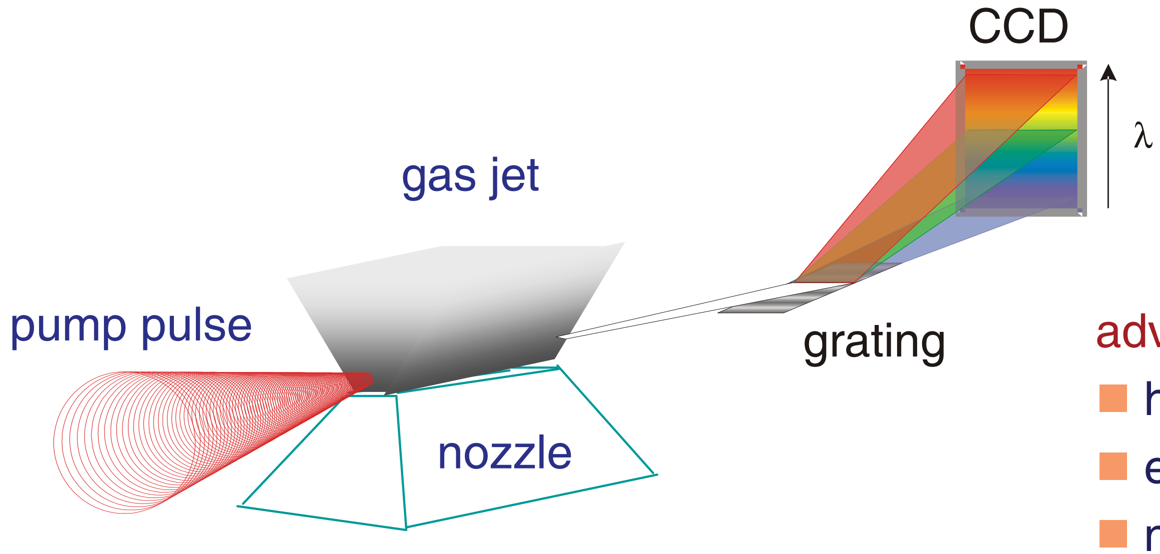

advantages:

- high efficiency
- excellent beam profile
- no debris

problem:

- ionization defocusing

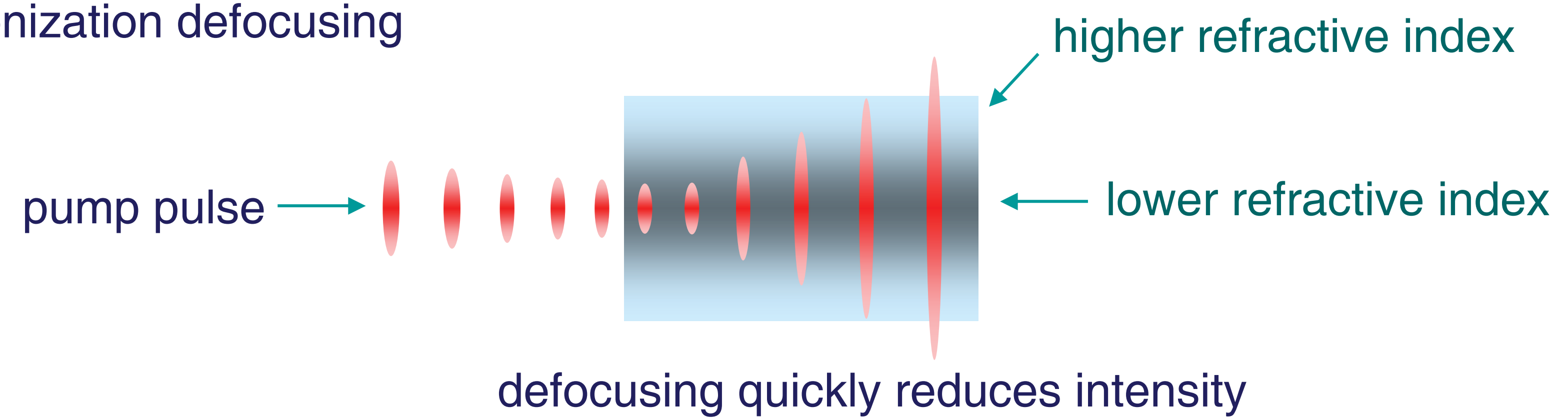

Interferograms of the plasma waveguide

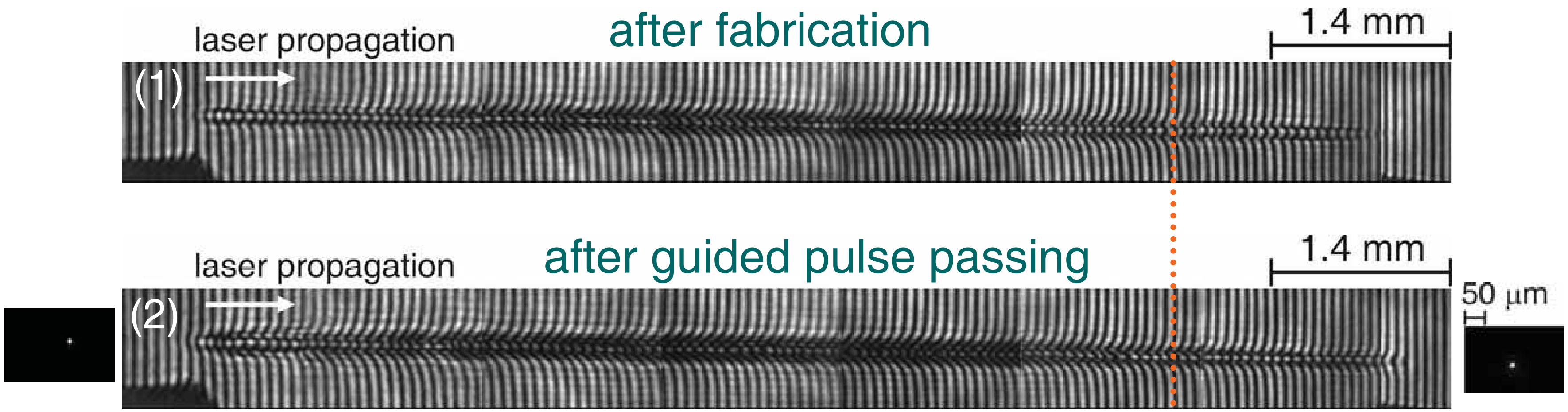

electron density distribution

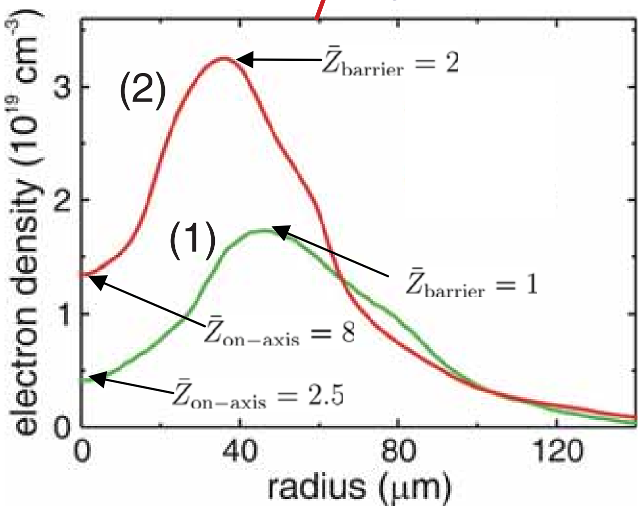

pump pulse: 45 fs, 235 mJ
ignitor: 45 fs, 45 mJ
heater: 80 ps, 225 mJ
ignitor-heater separation: 200 ps
hearer-pump delay: 2.5 ns
atom density: 1.6×10^{19} cm^{-3}

A uniform plasma waveguide of 40-μm diameter and 9-mm length is produced with the axicon-ignitor-heater scheme.

Pump-power dependence for Ni-like Kr lasing at 32.8 nm

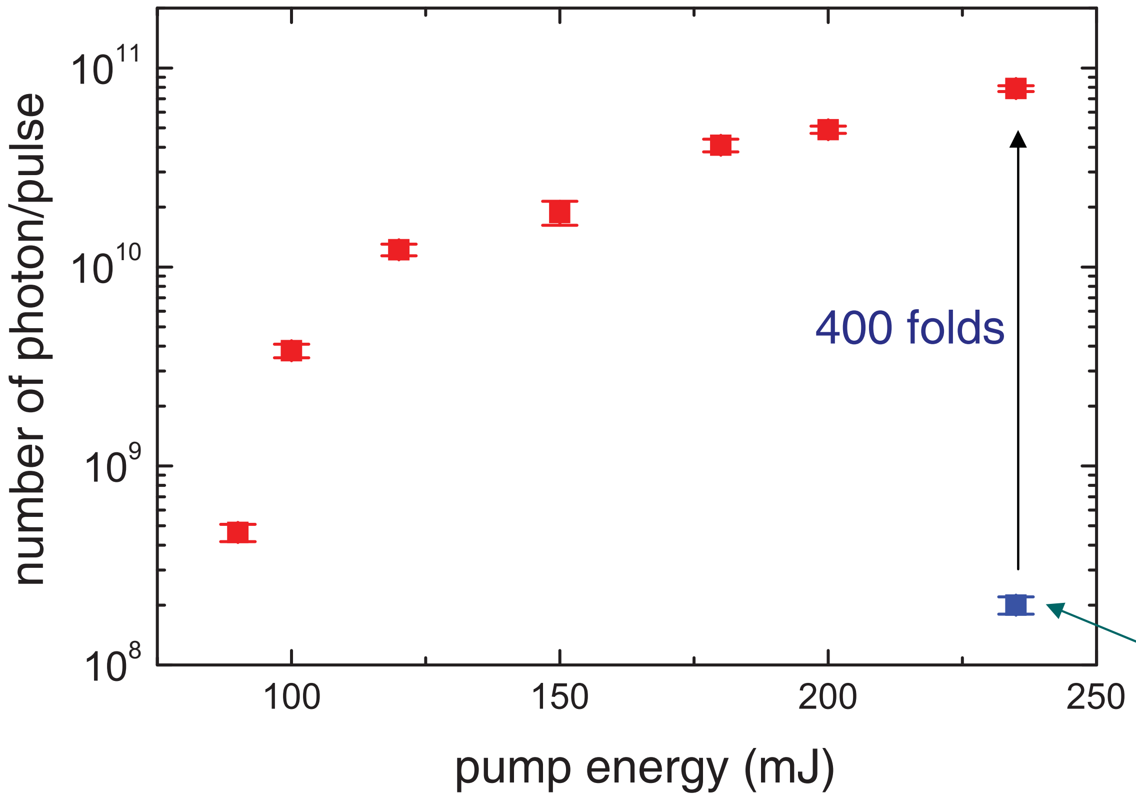

pure Kr waveguide
pump pulse: 45 fs
pump polarization: circular
focal position: 500 µm
ignitor: 45 fs, 45 mJ
heater: 80 ps, 225 mJ
ignitor-heater separation: 200 ps
heater-pump delay: 2.5 ns

optimized lasing without waveguide

Phys. Rev. Lett. **99**, 063904 (2007)

Reduced divergence

without waveguide

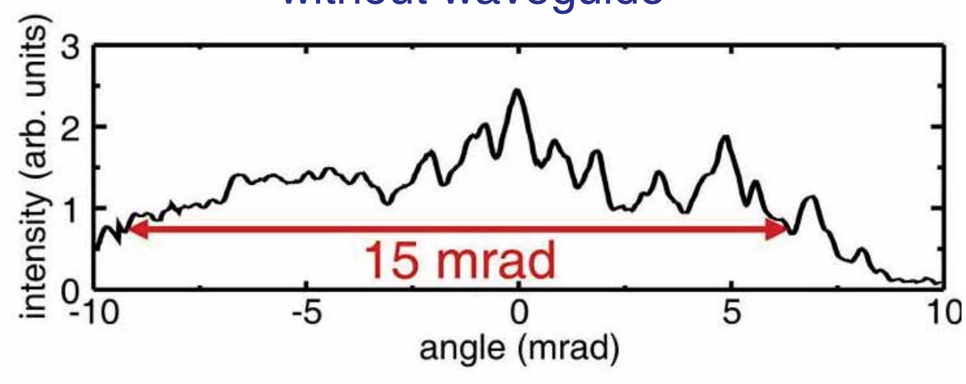

with waveguide

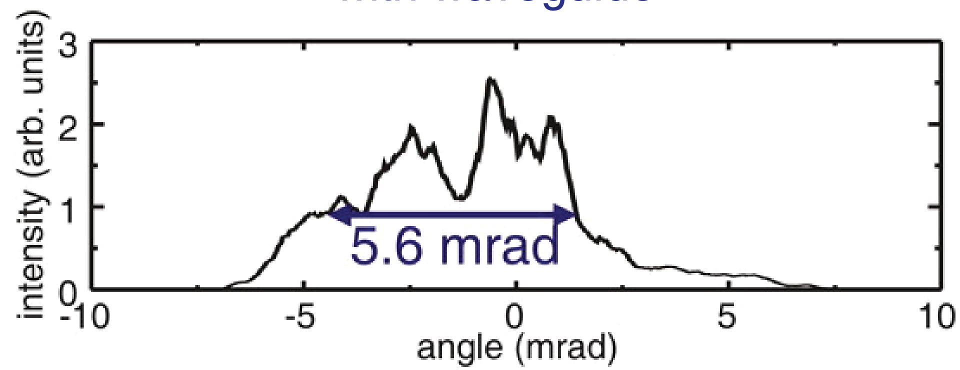

Phys. Rev. Lett. **99**, 063904 (2007)

Multi-line lasing for Ne-like Ar

raw image recorded by x-ray spectrometer

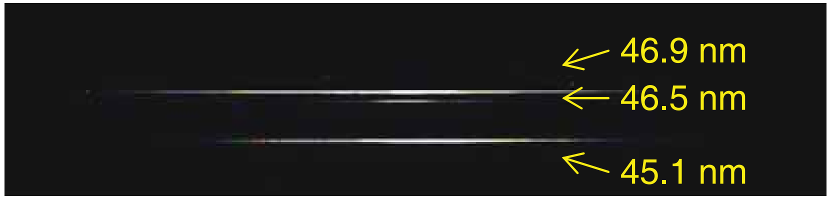

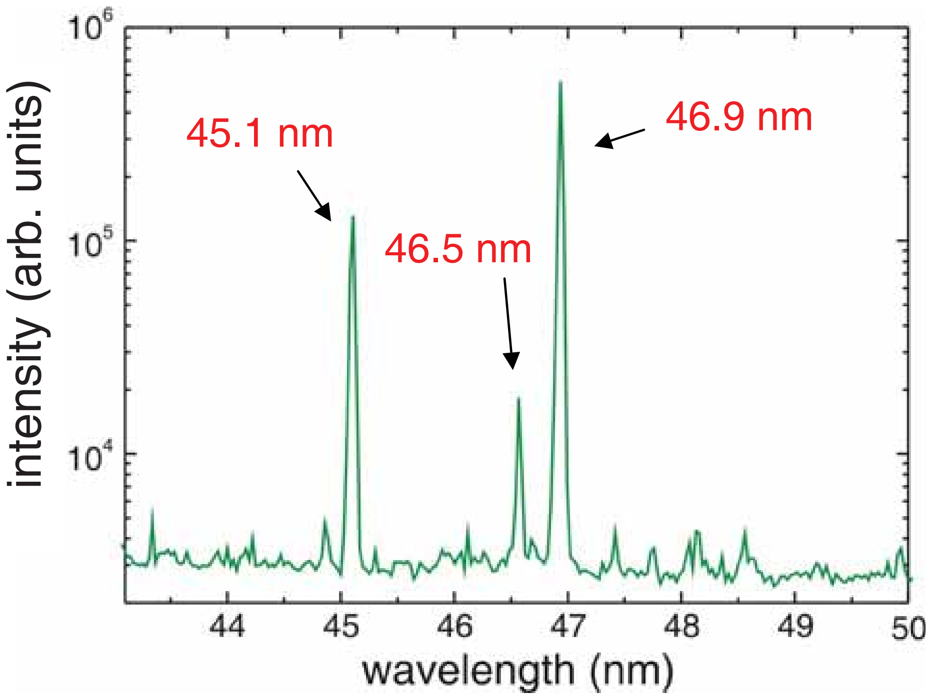

energy diagram of Ne-like Ar

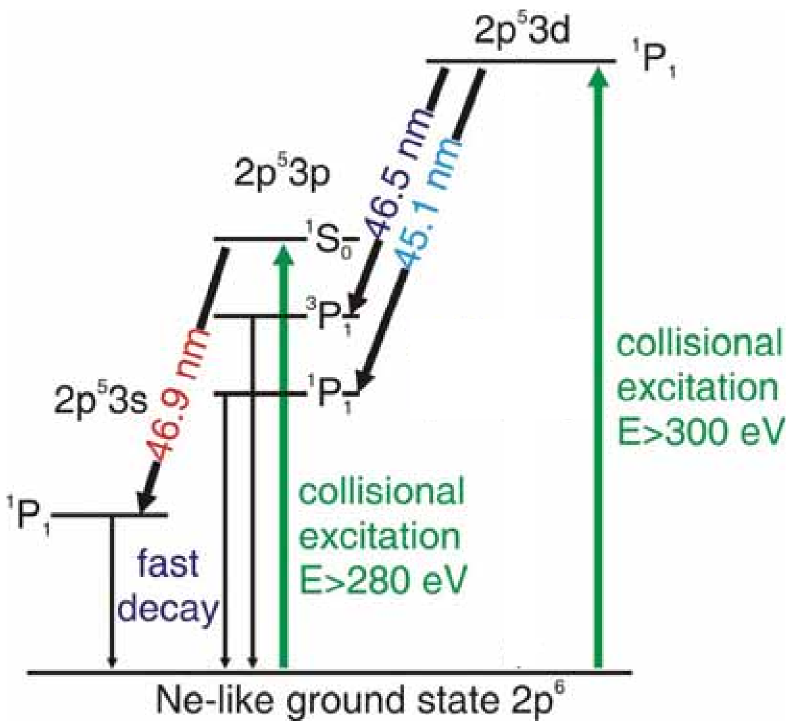

Phys. Rev. A **76**, 053817 (2007)

Multi-species parallel EUV lasing

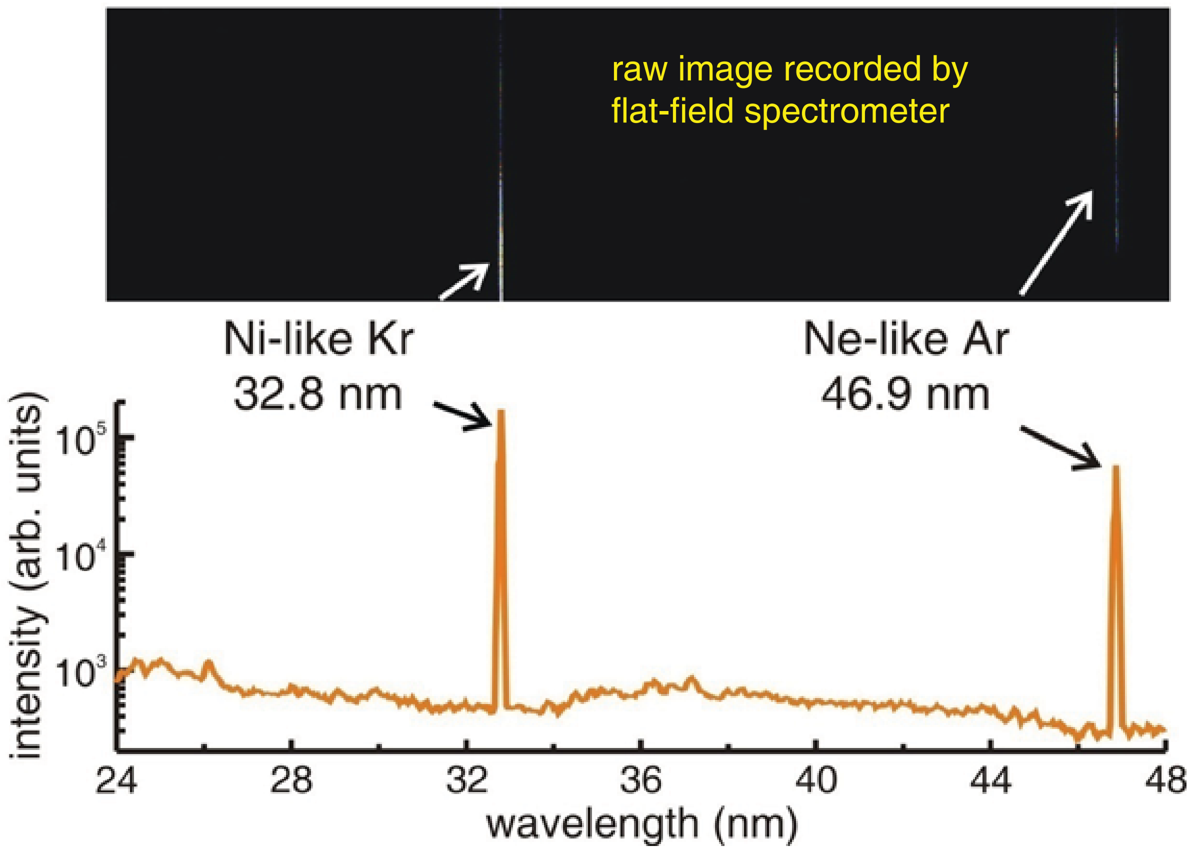

Kr/Ar mixed-gas waveguide
pump pulse: 45 fs, 240 mJ
pump polarization: circular
ignitor: 45 fs, 45 mJ
heater: 160 ps, 220 mJ
Kr atom density: 9.1×10^{18} cm^{-3}
Ar atom density: 1.2×10^{19} cm^{-3}
ignitor-heater separation: 200 ps
hearer-pump delay: 1.5 ns

gas mixture Kr : Ar = 0.9 : 1.2

Phys. Rev. A **76**, 053817 (2007)

Experimental setup for HHG injection seeding

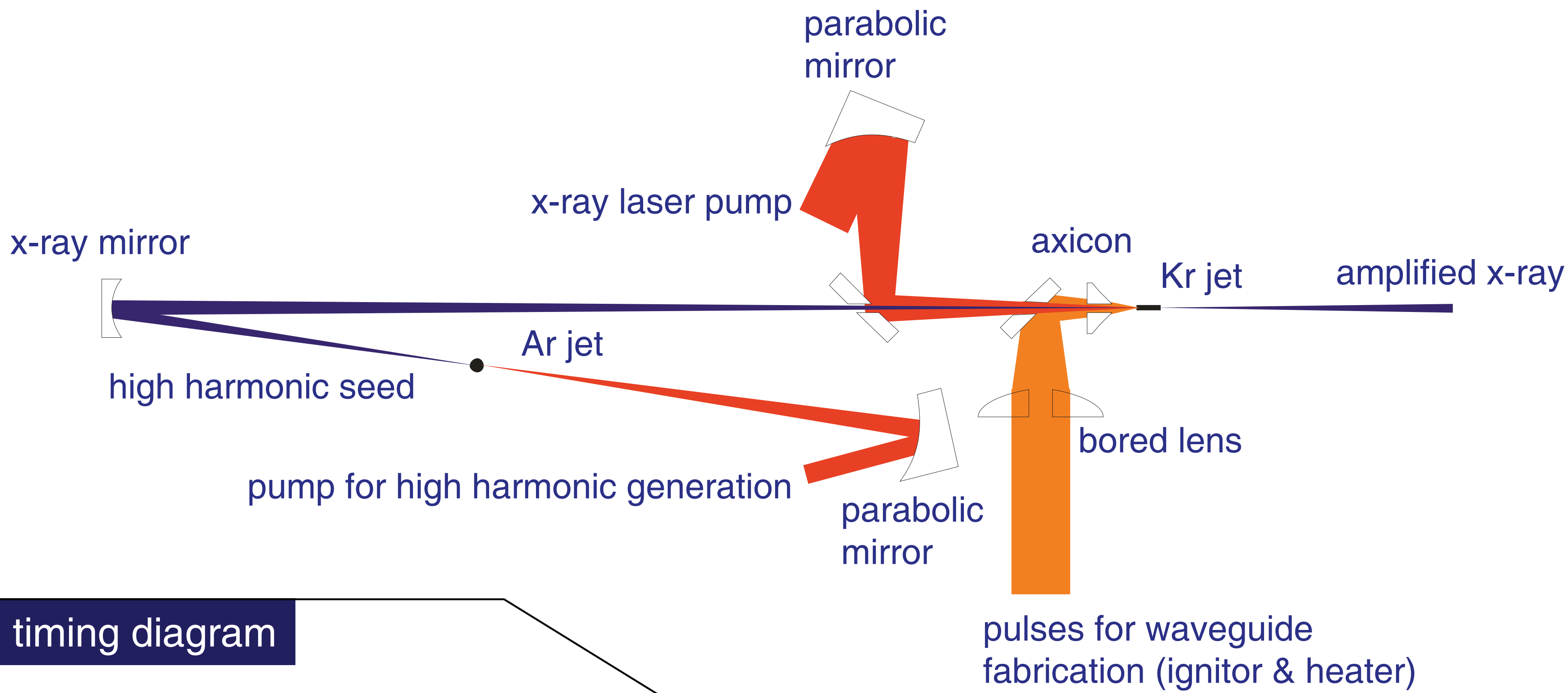

pulse timing diagram

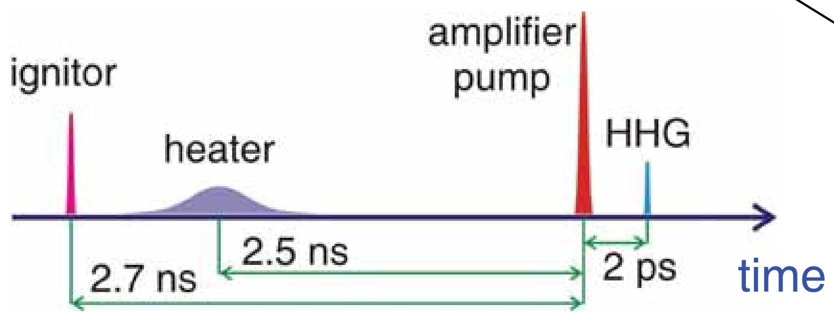

Opt. Lett. **34**, 3562 (2009)

Angular distribution of seeded EUV laser

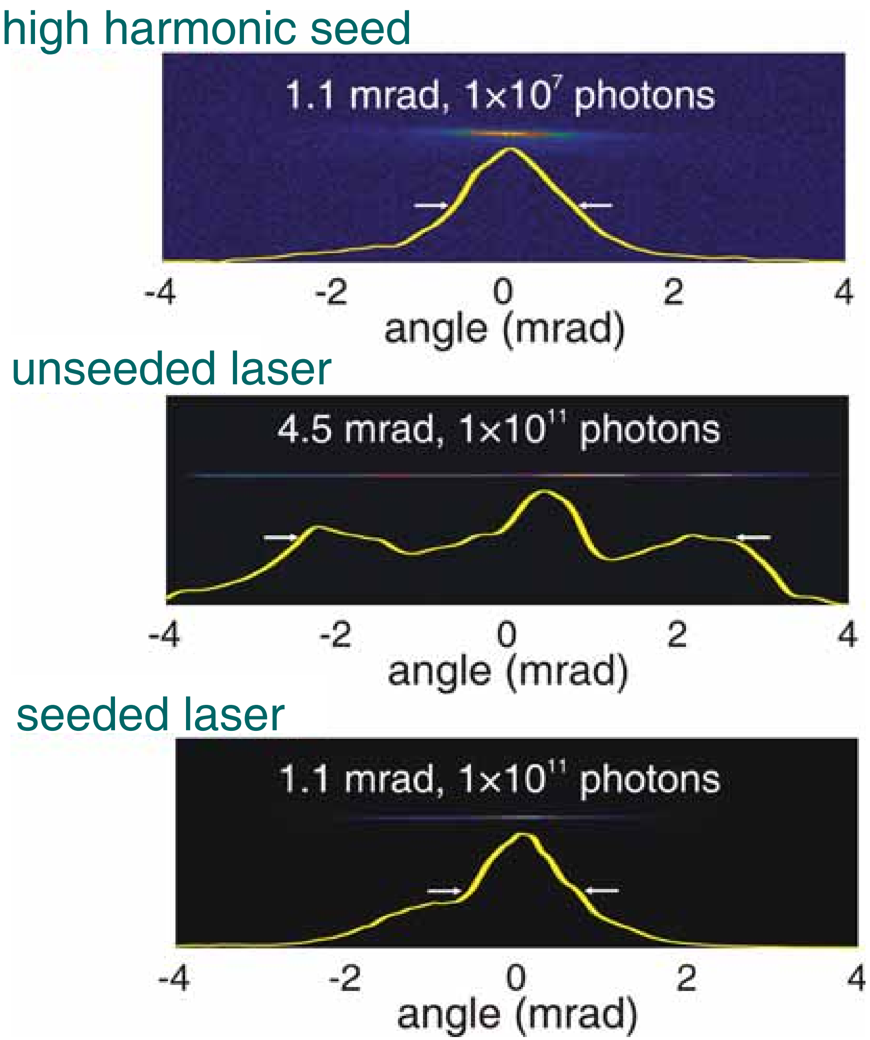

parameters of HHG seed:

gas: argon
atom density: 7.1×10^{18} cm^{-3}
pump energy: 3.8 mJ
pump duration: 360 fs
focal position: 1250 μm
seed-amplifier pump delay: 2 ps

parameters of x-ray amplifier:

gas: krypton
atom density: 1.6×10^{19} cm^{-3}
pump pulse: 38 fs, 235 mJ
ignitor: 38 fs, 45 mJ
heater: 160 ps, 270 mJ
ignitor-heater separation: 200 ps
heater-pump delay: 2.5 ns

beam-pointing fluctuation: 0.13 mrad

energy fluctuation: 10%

- With seeding the divergence of the x-ray laser is greatly reduced from 4.5 mrad to 1.1 mrad, which is about the same as that of the HHG seed.
- With the waveguide-based soft-x-ray amplifier, the HHG seed is amplified by a factor of 10^4.

Output energy of Ni-like Kr laser

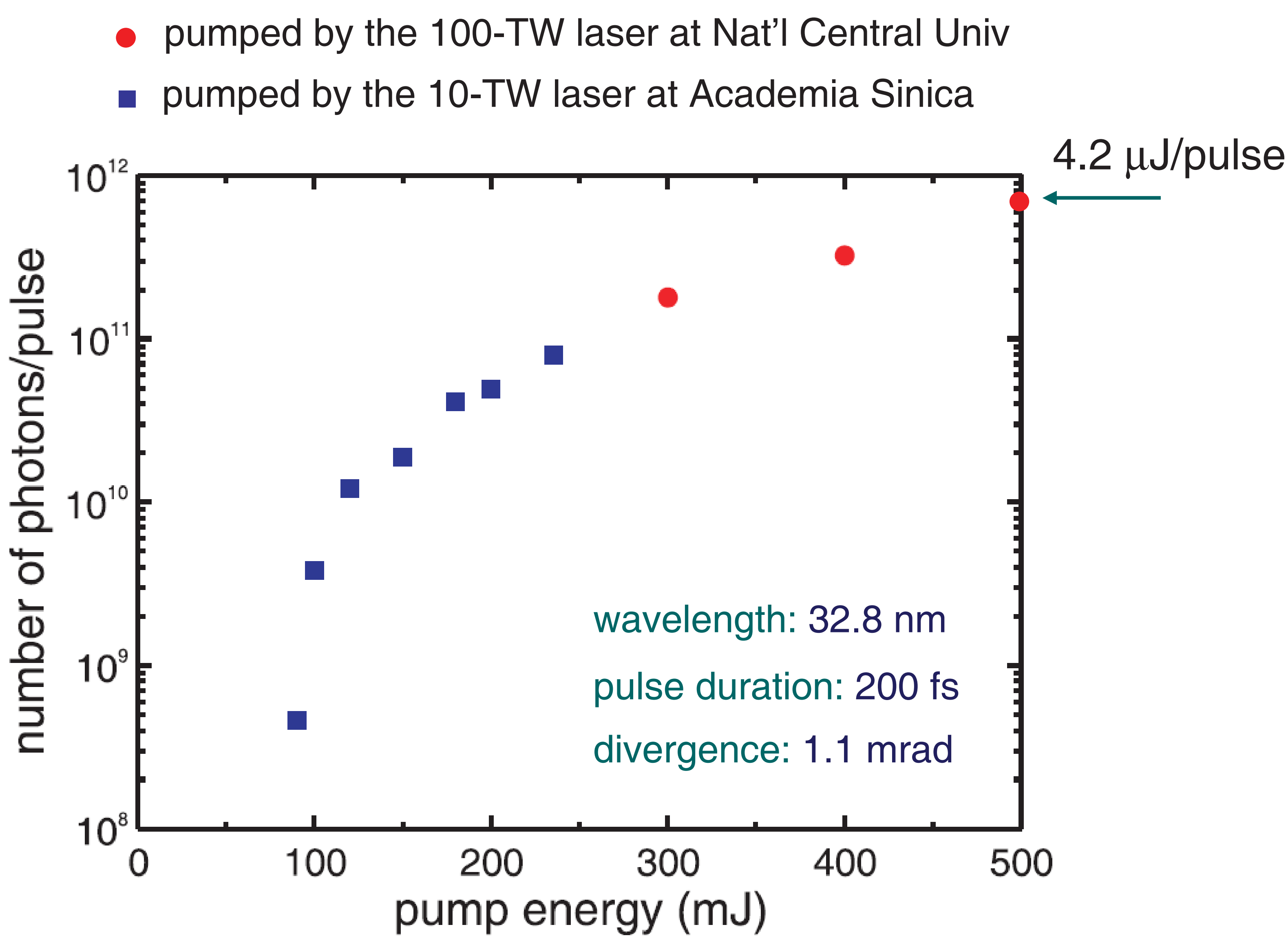

Comparing our EUV laser with synchrotron radiation

spectral brightness (photon/sec/mm^2/mrad^2) for $\frac{\Delta\lambda}{\lambda} = 10^{-3}$

	NSRRC (Taiwan)	x-ray laser (HHG seeding)
pulse duration	100 ps	200 fs*
repetition rate	10^6 Hz	10 Hz
wavelength	tunable	discrete set
average spectral brightness at 32.8 nm	9.8×10^{13}	6.6×10^{14}
peak spectral brightness at 32.8 nm	5.8×10^{17}	2.9×10^{28}

* assuming the pulse duration is limited by bandwidth

Laser-wakefield electron accelerator

Phys. Rev. Lett. **96**, 095001 (2006)

Phys. Rev. E **75**, 036402 (2007)

Phys. Plasmas **18**, 063102 (2011)

The 27-km ring accelerator at CERN

material break-down limit of conventional accelerator: 10^8 V/m

Proposal of laser-plasma accelerator

NUMBER 4 PHYSICAL REVIEW LETTERS 23

Laser Electron Accelerator

T. Tajima and J. M. Dawson
Department of Physics, University of California, Los Angeles, California 90024
(Received 9 March 1979)

An intense electromagnetic pulse can create a weak of plasma oscillations through the action of the nonlinear ponderomotive force. Electrons trapped in the wake can be accelerated to high energy. Existing glass lasers of power density 10^{18}W/cm^2 shone on plasmas of densities 10^{18} cm^{-3} can yield gigaelectronvolts of electron energy per centimeter of acceleration distance. This acceleration mechanism is demonstrated through computer simulation. Applications to accelerators and pulsers are examined.

Laser-wakefield electron accelerator

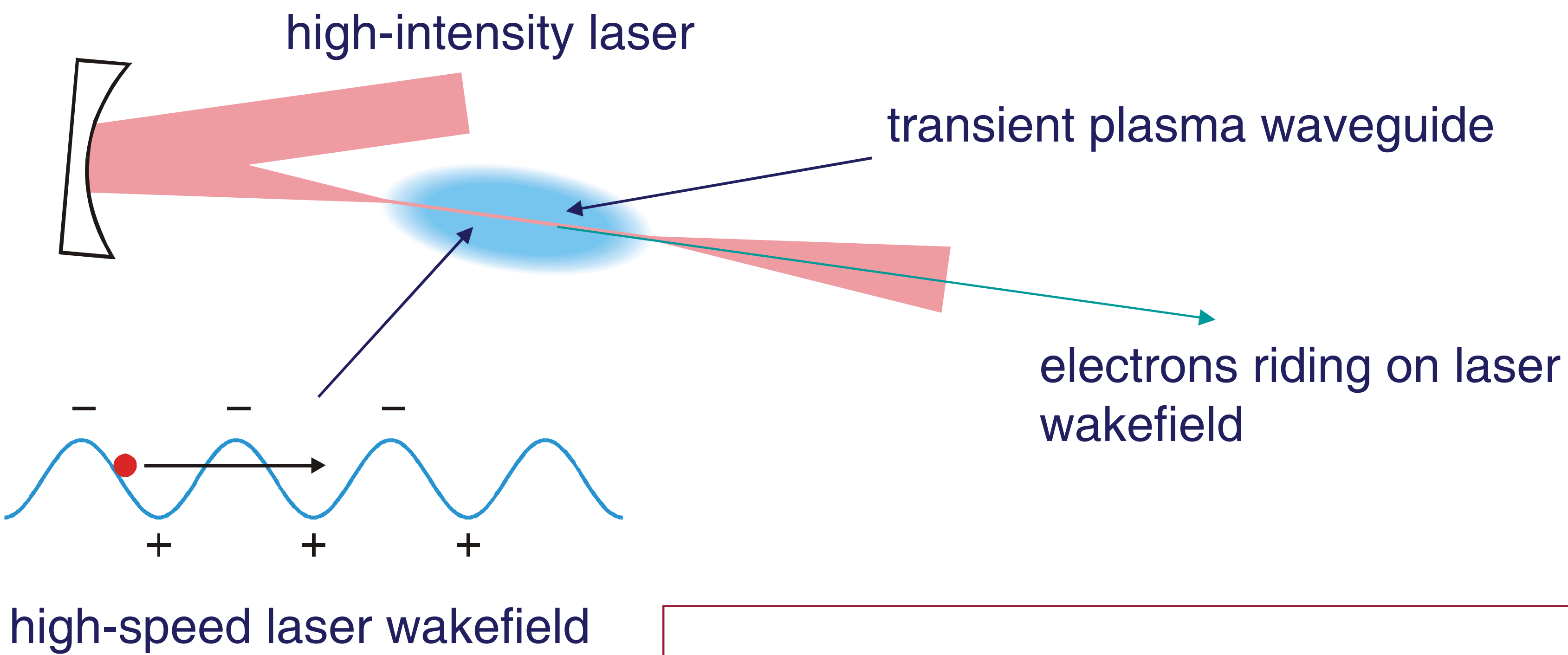

acceleration gradient: 250 GeV/m

conventional accelerator: 50 MeV/m

Acceleration in the "bubble regime"

evolution of laser pulse

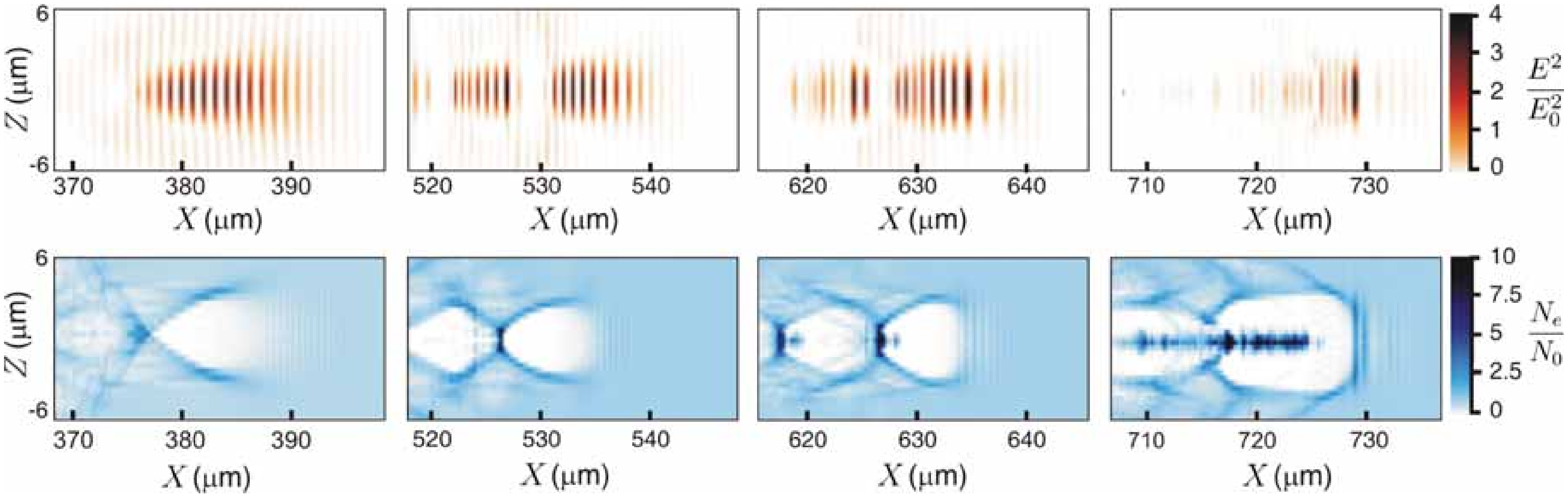

evolution of electron density

- After nonlinear propagation, pulse duration becomes smaller than plasma-wave period.
- The ponderomotive force expels electrons, resulting in a positively charged cavity following laser pulse.

Production of a monoenergetic electron beam

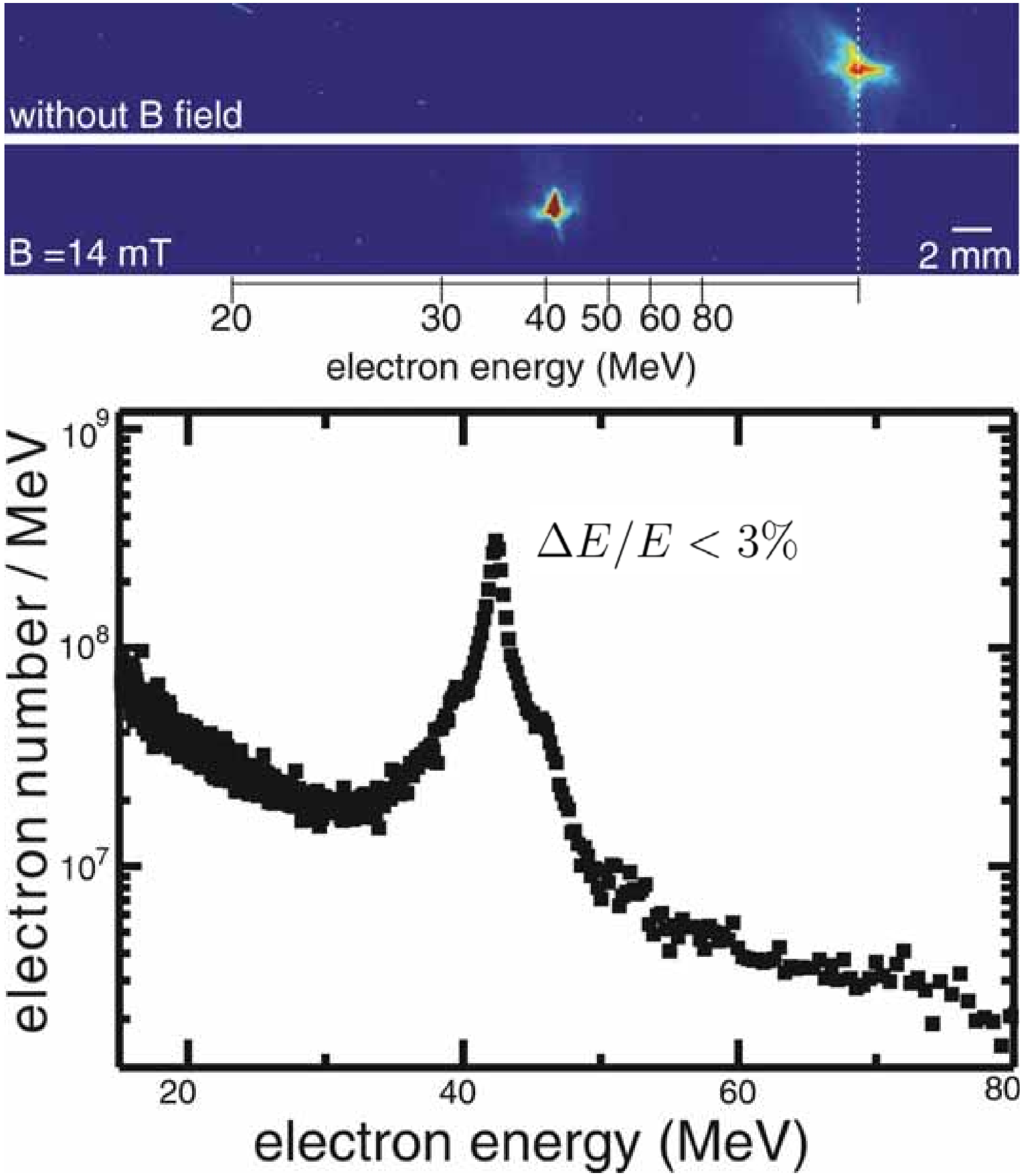

plasma density:

4×10^{19} cm^{-3}

pump pulse:

230 mJ, 45 fs,

focused to 8-μm diameter

Phys. Rev. Lett. **96**, 095001 (2006)

Electron images at the spectrometer

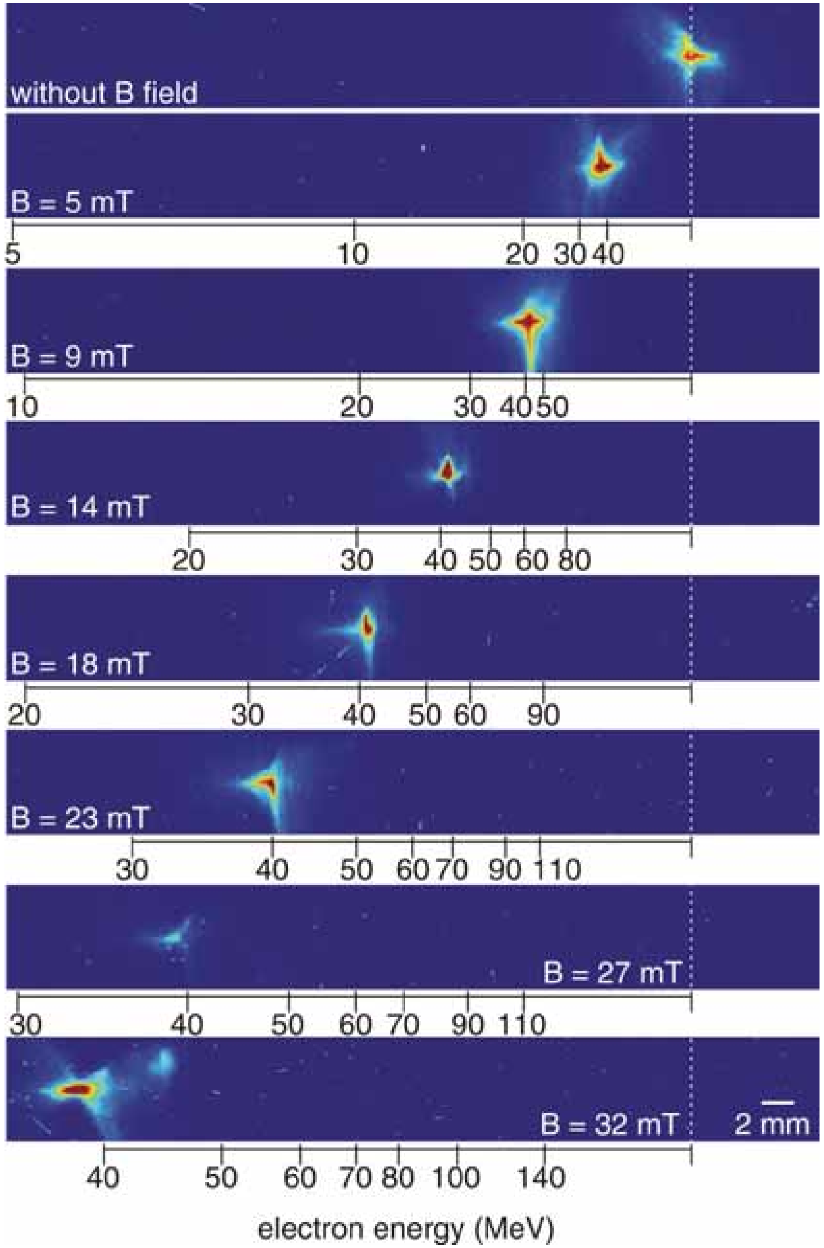

Resolving the acceleration process

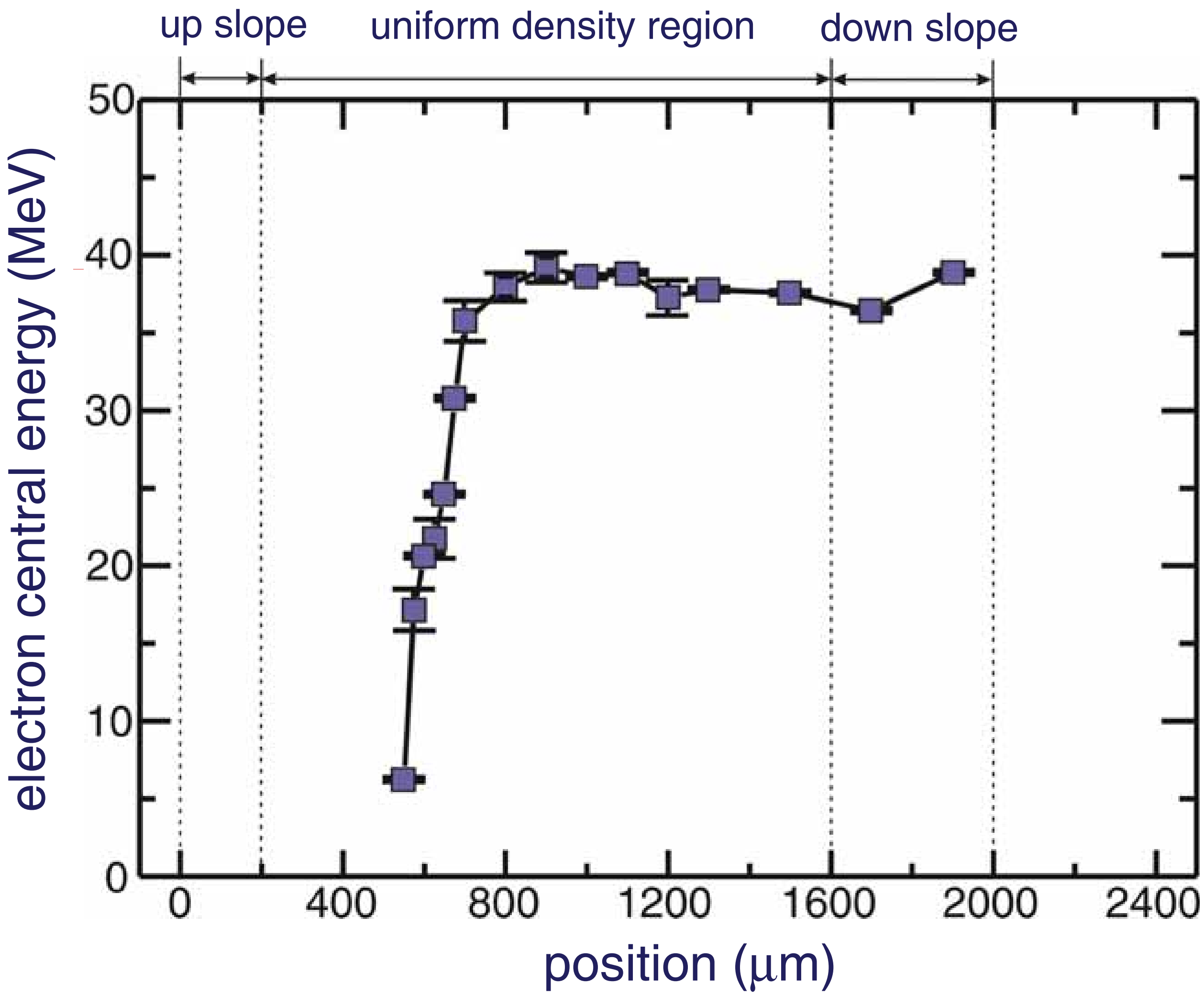

- Saturation of electron energy occurs at ~200-μm acceleration distance.
- The first direct measurement of the acceleration gradient (~2 GeV/cm).

Phys. Rev. E **75**, 036402 (2007)

Acceleration in optically preformed waveguide

advantages:

- gas jet based waveguide, no accumulated damage
- independent adjustment of plasma density and laser parameters

guided pump pulse:
1.3 J, 35 fs ,
intensity: 2.3×10^{19} W/cm^2

guiding throughput:
90% (small energy)

waveguide forming pulse:
ignitor, 90 mJ
heater, 280 mJ
ignitor-heater separation: 400 ps
heater-pump delay 1.5 ns

on-axis electron density:
3.2×10^{18} cm^{-3}

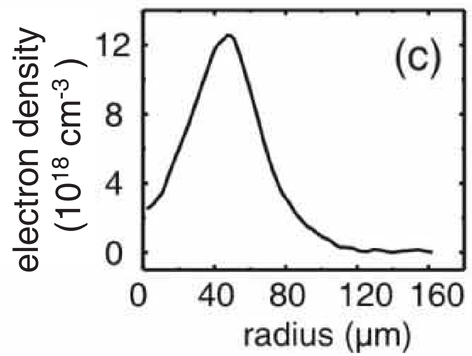

Electron beam profile and energy spectrum

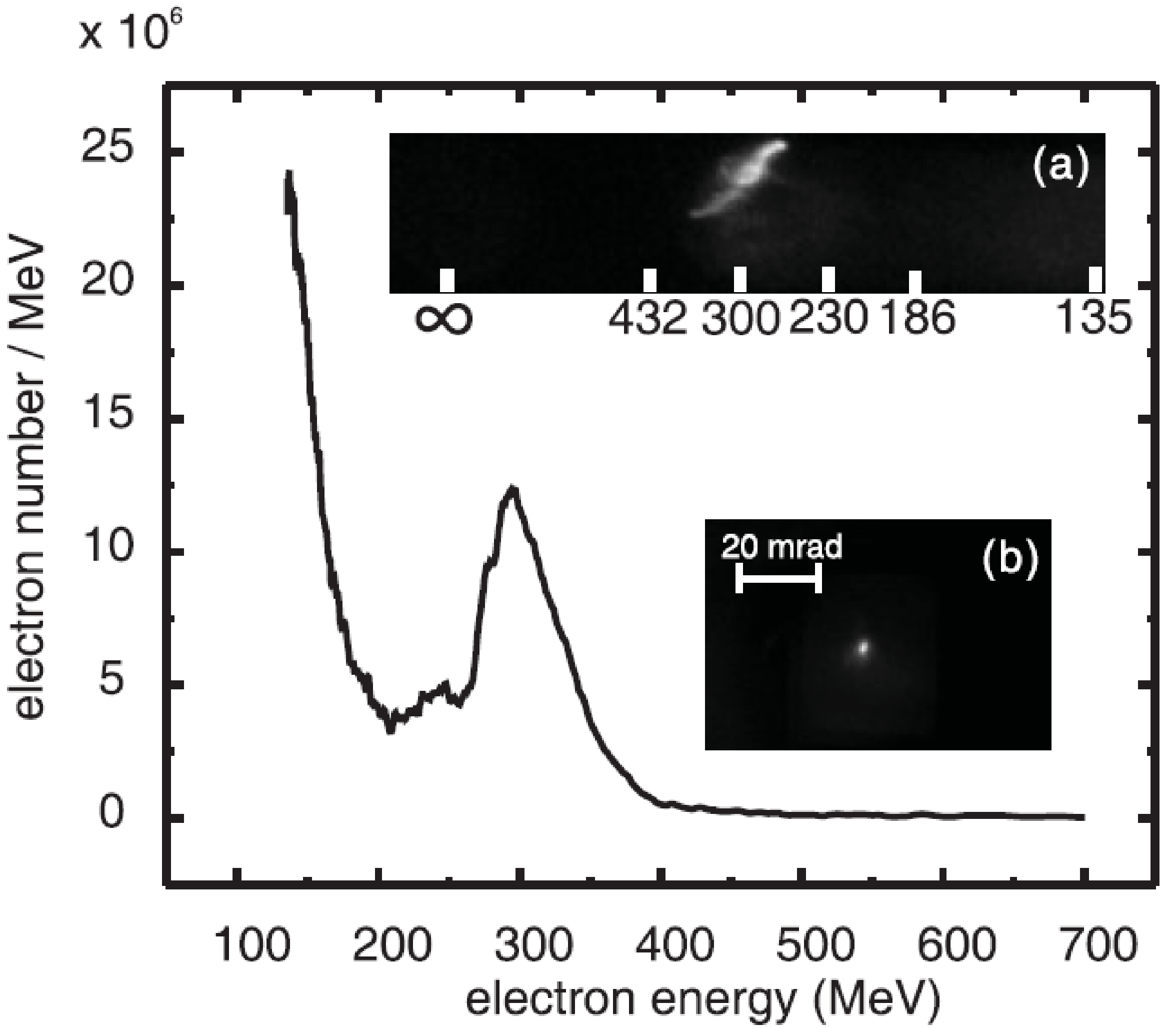

pump pulse: 1.3 J

electron energy: 300 MeV

bunch charge: 200 pC (best case)

divergence: 2.5 mrad

ΔE/E: 13%

Phys. Plasmas **18**, 063102 (2011)

27 years after the proposal

Lawrence Berkeley National Laboratory

Published online: 24 September 2006; doi:10.1038/nphys418

Gigaelectron volt (GeV) electron accelerators are essential to synchrotron radiation facilities and free-electron lasers, and as modules for high-energy particle physics. Radiofrequency-based accelerators are limited to relatively low accelerating fields (10–50 MV m^{-1}), requiring tens to hundreds of metres to reach the multi-GeV beam energies needed to drive radiation sources, and many kilometres to generate particle energies of interest to high-energy physics. Laser-wakefield accelerators[1,2] produce electric fields of the order 10–100 GV m^{-1} enabling compact devices. Previously, the required laser intensity was not maintained over the distance needed to reach GeV energies, and hence acceleration was limited to the 100 MeV scale[3–5]. Contrary to predictions that petawatt-class lasers would be needed to reach GeV energies[6,7], here we demonstrate production of a high-quality electron beam with 1 GeV energy by channelling a 40 TW peak-power laser pulse in a 3.3-cm-long gas-filled capillary discharge waveguide[8,9].

bunch charge: only 30 pC

Relativistic plasma nonlinear optics

Phys. Rev. A **76**, 063815 (2007)

Phys. Rev. Lett. **98**, 033901 (2007)

Phys. Rev. A **82**, 063804 (2010)

Phys. Rev. A **83**, 033801 (2011)

Relativistic nonlinearity in laser plasma interaction

- Relativistic effects on plasma refractive index

$$\Delta n = \sqrt{1 - \frac{{\omega_p}^2}{\omega^2 \sqrt{1 + a^2/2}}} - \sqrt{1 - \frac{{\omega_p}^2}{\omega^2}}$$

relativistic self-phase modulation

- Wave mixing mediated by plasma waves
- Relativistic nonlinearity of the Lorentz force

$$\mathbf{F} = e\left(\mathbf{E} + \frac{\mathbf{v}}{c} \times \mathbf{B}\right)$$

nonlinear force

Theoretic analysis of the electron motion

$$\mathbf{a} \equiv \frac{|e|\mathbf{A}}{m_e c^2} \qquad \phi \equiv \frac{|e|\Phi}{m_e c^2}$$

normalized vector and scalar potentials

$$\frac{d\mathbf{p}}{dt} = m_e c^2 \left[\frac{1}{c} \frac{\partial \mathbf{a}}{\partial t} + \nabla \phi - \boldsymbol{\beta} \times (\nabla \times \mathbf{a}) \right]$$

Lorentz force

$$\nabla^2 \phi = k_p^2 \left(\frac{n_e}{n_0} - 1 \right)$$

Poisson's Equation

$$\frac{\partial n_e}{\partial t} + c \nabla \cdot (n_e \boldsymbol{\beta}) = 0$$

Continuity Equation

$\mathbf{a}$: known laser field

solution $\longrightarrow$ ϕ, $\boldsymbol{\beta}$, n_e

Modification of the laser field

$$\left(\nabla^2 - \frac{\partial^2}{c^2\partial t^2}\right)\mathbf{a} = k_p^2\,\frac{n_e}{n_0}\,\boldsymbol{\beta} + \frac{\partial \nabla \phi}{c\partial t}$$ Maxwell Equation

nonlinear source terms (functions of $\mathbf{a}$)

0-ω source term → optical rectification

1-ω source term → nonlinear refractive index

n-ω source term → harmonic generation

Relativistic second harmonic generation

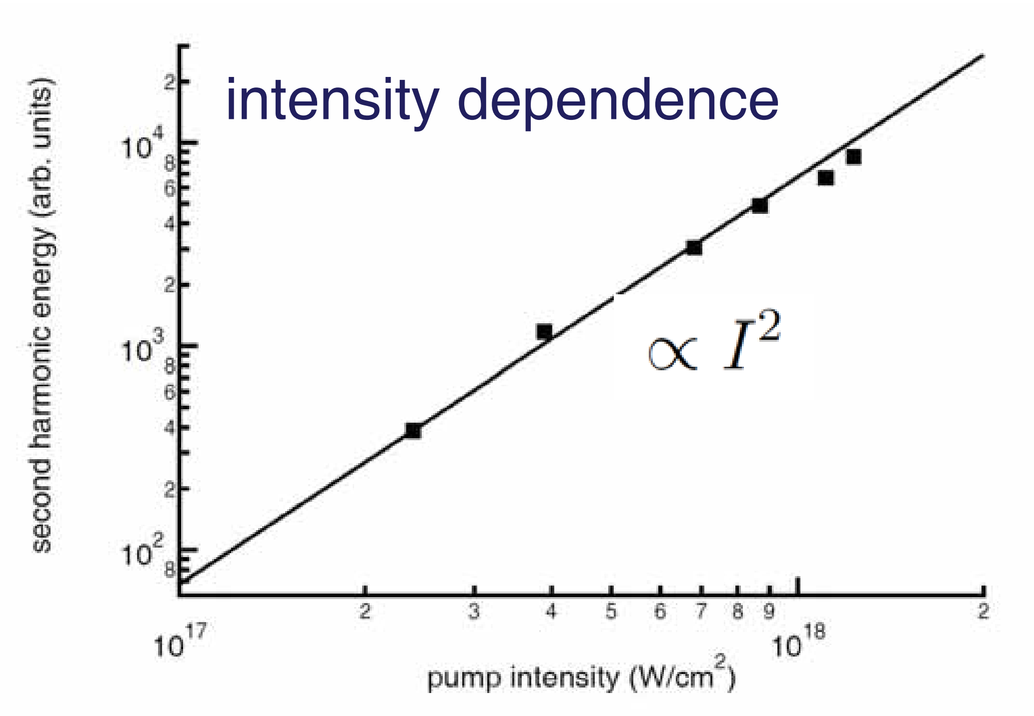

— theory

■ ■ ■ experiment

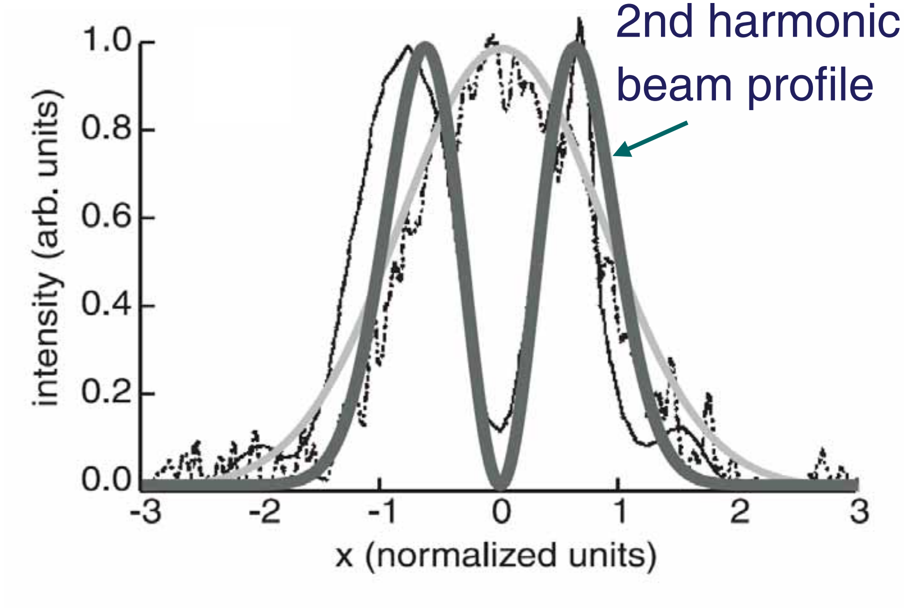

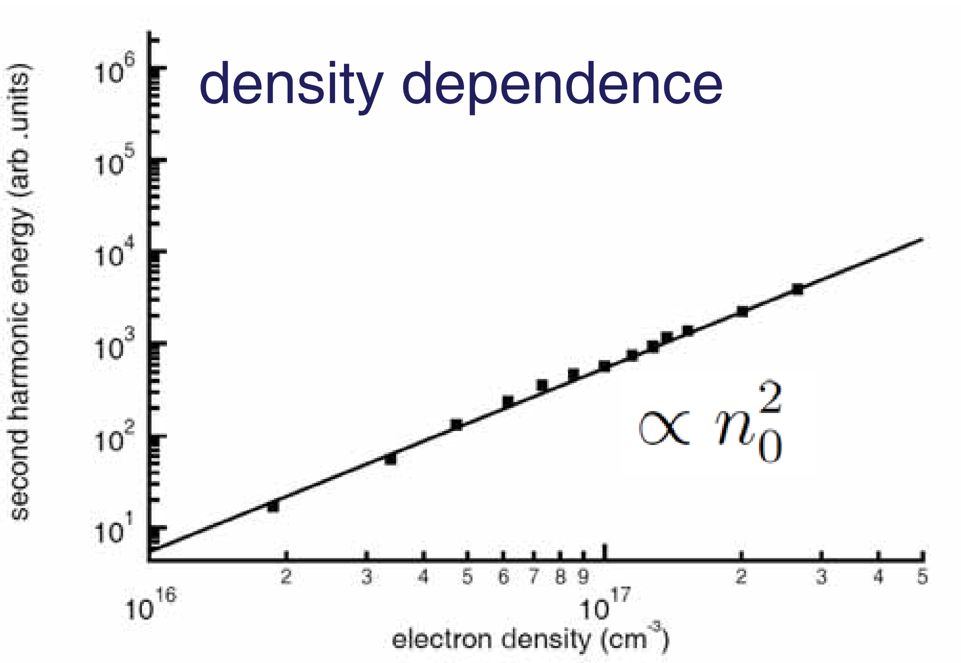

Phys. Rev. A **76**, 063815 (2007)

Generation of few-cycle intense mid-infrared pulses

Phys. Rev. A **82**, 063804 (2010)

Nonlinear phase modulation in the bubble regime

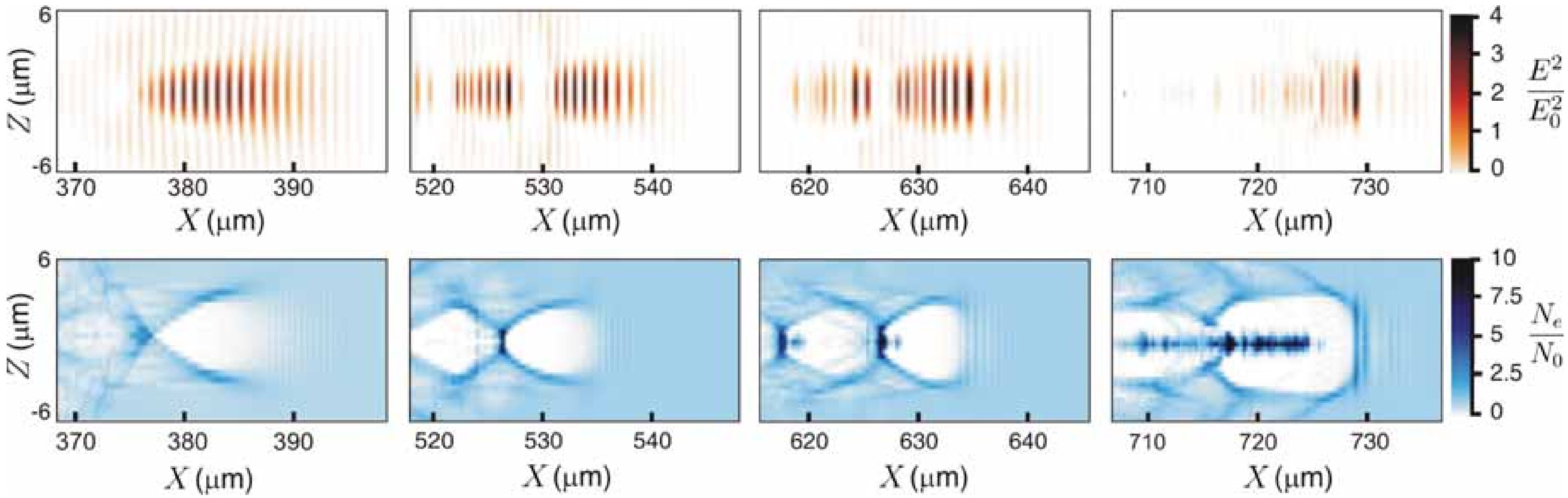

modulation of refractive index

density modulation

$$\Delta n = \sqrt{1 - \frac{{\omega_p}^2}{\omega^2 \sqrt{1 + a^2/2}}} - \sqrt{1 - \frac{{\omega_p}^2}{\omega^2}}$$

relativistic self-phase modulation

advantages:

- no optical damage
- large working bandwidth
- high spatial coherence

Ge-wafer photo-switch

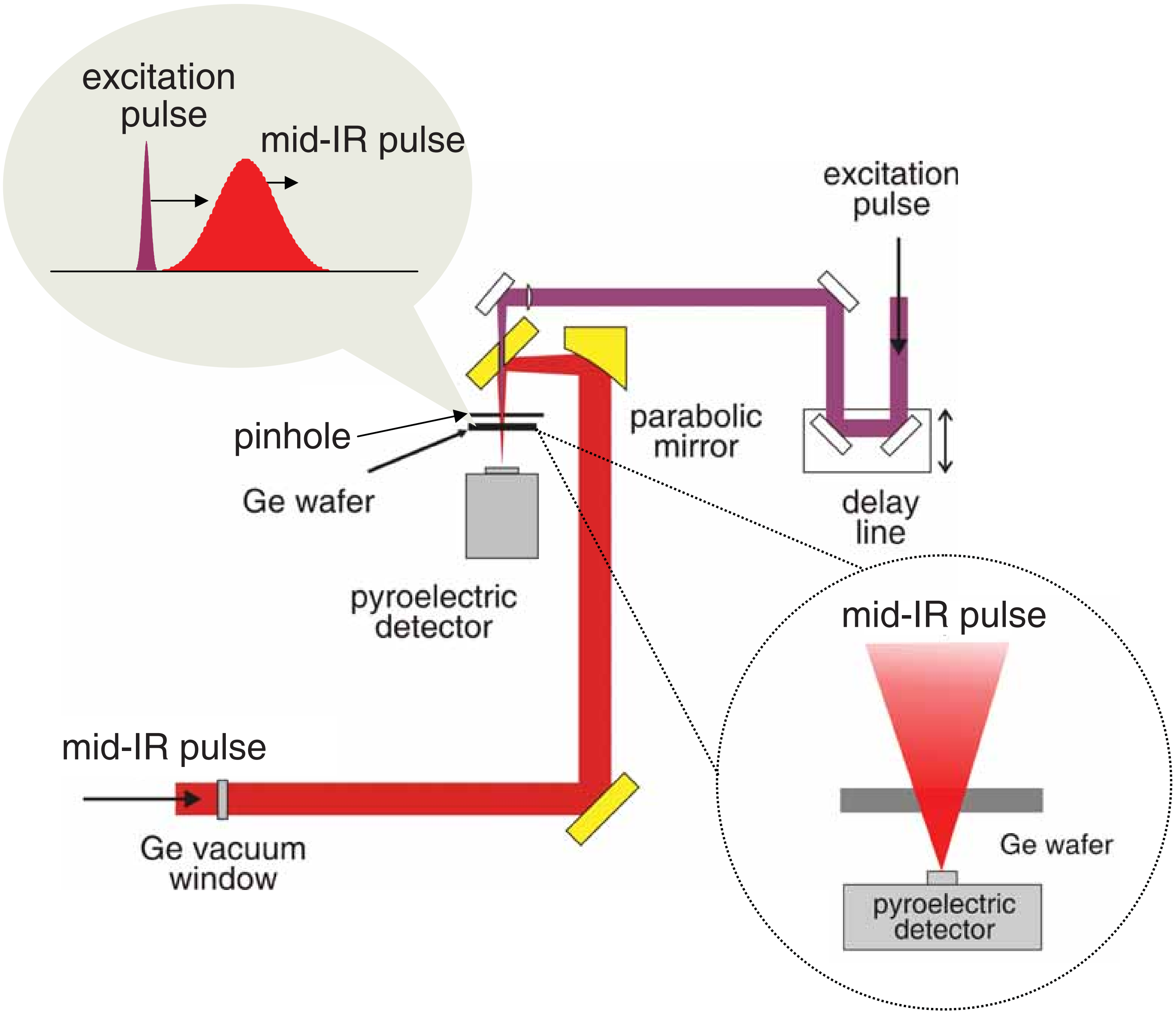

Ge-wafer photo-switch

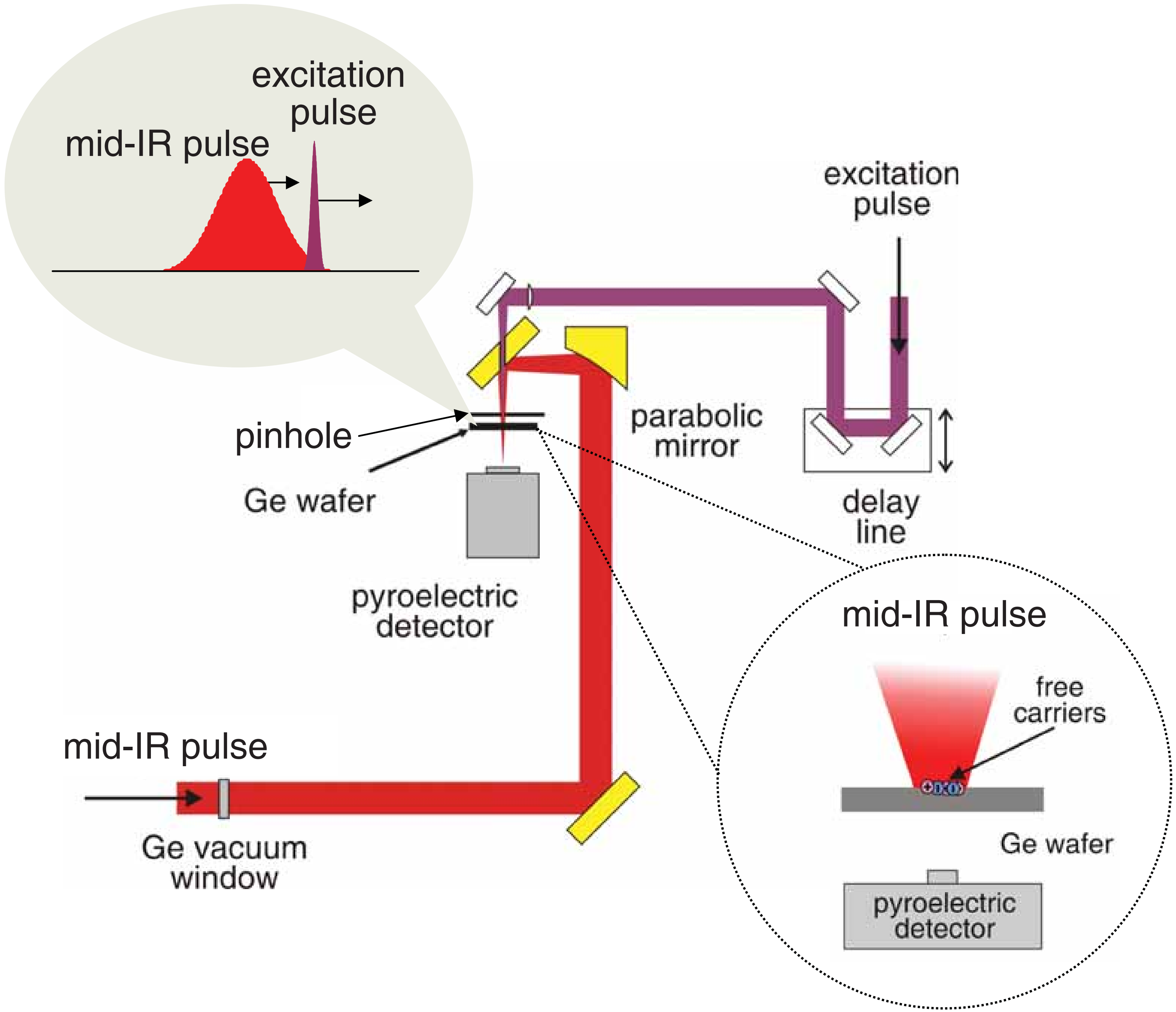

Temporal profile of the mid-IR pulse

photo-switch gated transmission

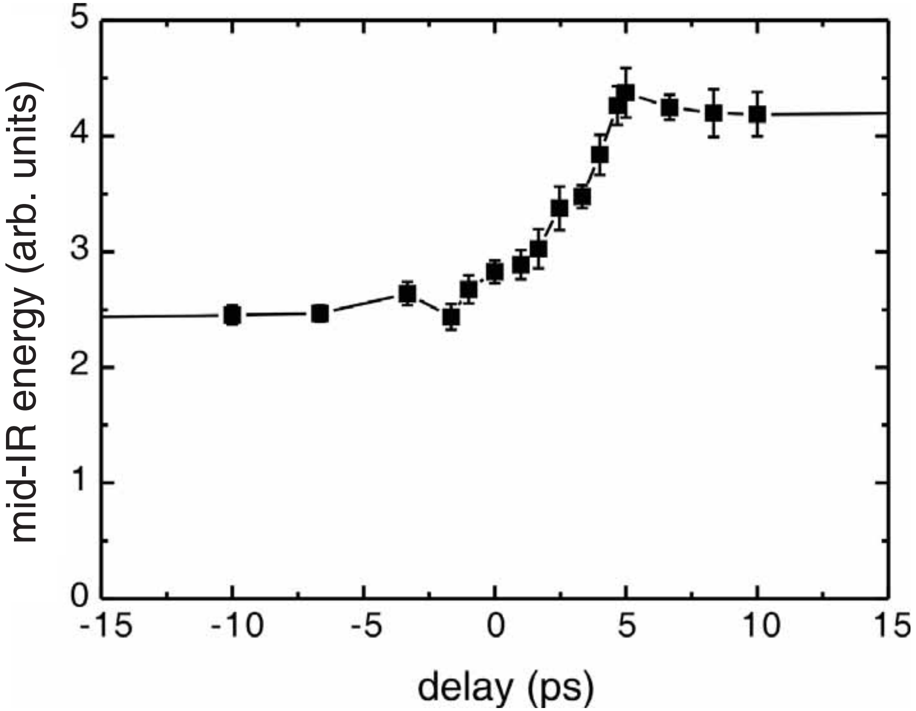

reconstructed temporal profile

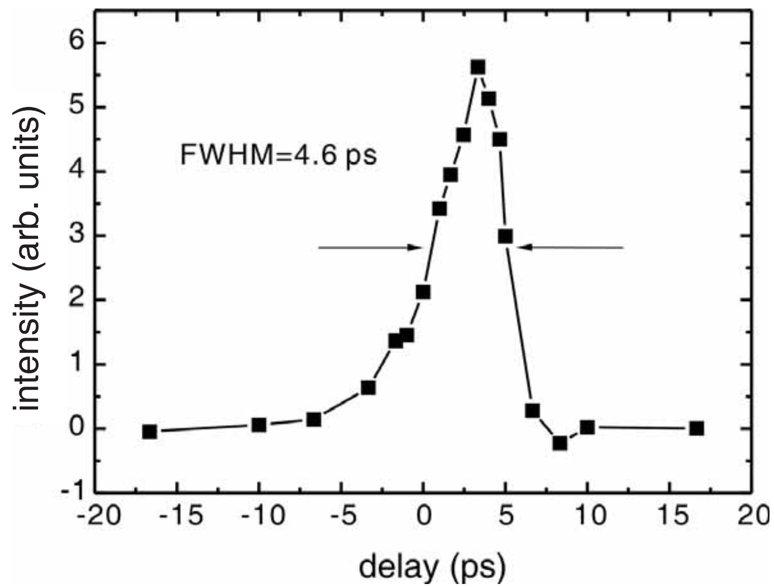

pump pulse: 205 mJ/42 fs
excitation pulse: 500 μJ/38 fs
plasma density: 4.1×10^{19} cm^{-3}

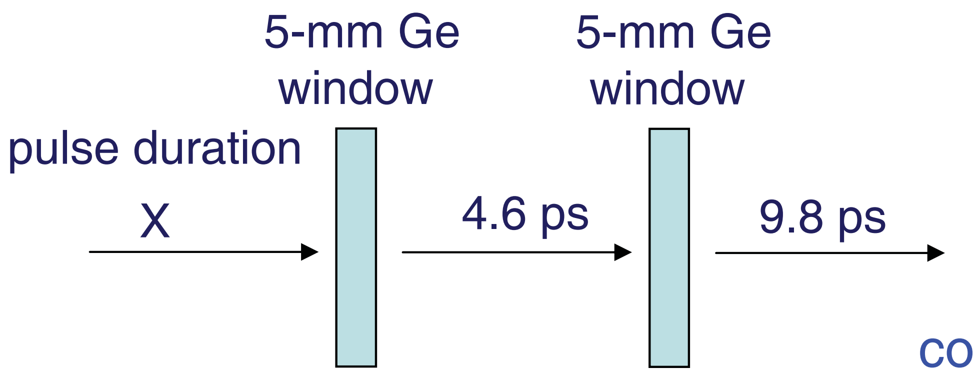

X～15 fs

consistent with particle-in-cell simulation

Comparing with simulation and theoretical estimation

Estimation based on Fourier transform of the phase modulated pulse

Square of the electric field of the numerically filtered mid-IR pulse

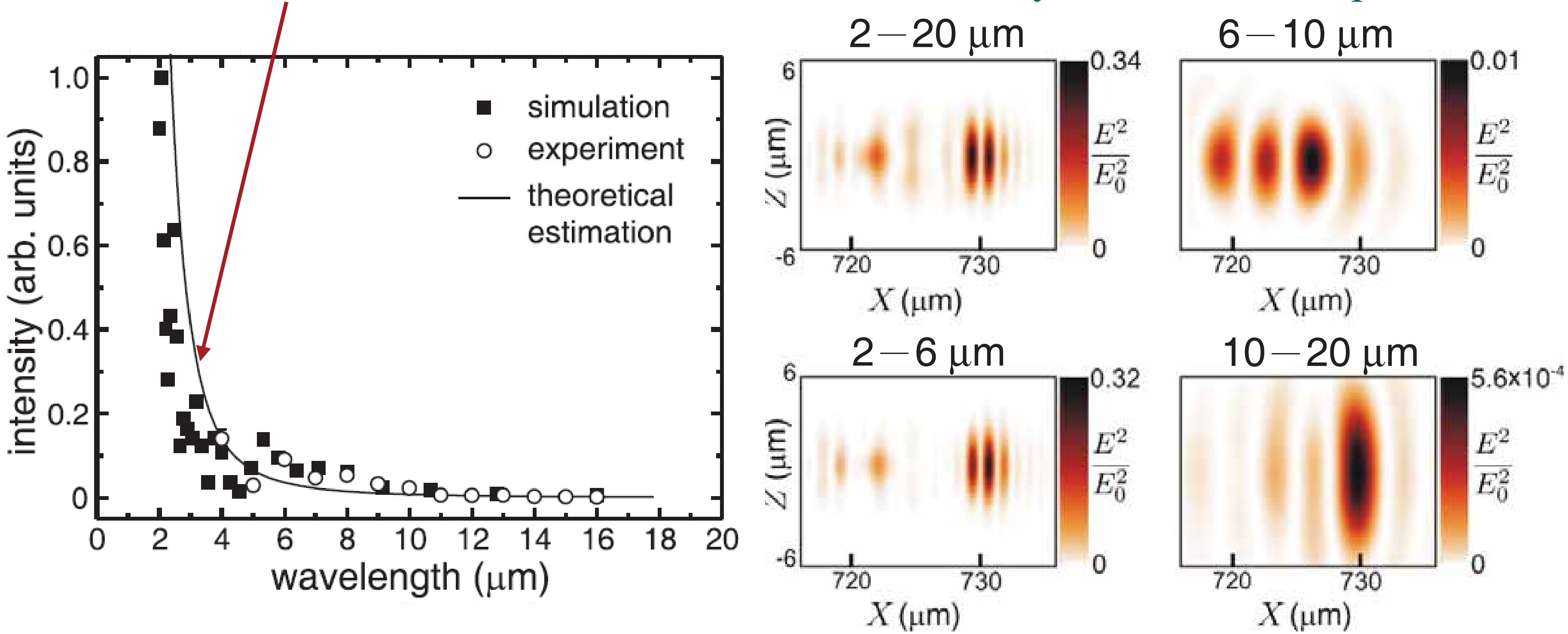

- Energy: 7 mJ, duration 12 fs, mid-IR peak power in the bubble: > 0.5 TW
- The mid-IR pulse is encapsulated in the low-density bubble, hence is not absorbed by the plasma. The wavelength-scale bubble ensures high spatial coherence.

Relativistic induced birefringence

Phys. Rev. A **83**, 033801 (2011)

Two-beam interaction via plasma waves

$$a_x = a\sin(k\zeta) + \frac{a'}{\sqrt{2}}\sin(k'\zeta')$$

$$a_y = \frac{a'}{\sqrt{2}}\sin(k'\zeta')$$

$$a_z = 0$$

$\zeta = \eta z - ct, \quad \zeta' = \eta' z - ct$

$\eta,\ \eta'$: refractive index

$a' \ll a$

$$\left(\nabla^2 - \frac{\partial^2}{c^2\partial t^2}\right)\mathbf{a} = k_p^2 \frac{n_e}{n_0}\boldsymbol{\beta} + \frac{\partial \nabla \phi}{c\partial t}$$ Maxwell Equation

nonlinear source terms (functions of $\mathbf{a}$)

a and a' create plasma waves of $k \pm k'$, which scatter a_x into a_x'.

induced birefringence

$$\eta_y' - \eta_x' \approx \frac{k_p^4 a^2}{8(1+a^2/2)^2 k'^2}\left[\frac{1}{(k+k')^2} + \frac{1}{(k-k')^2}\right]$$

Verified by particle-in-cell simulation

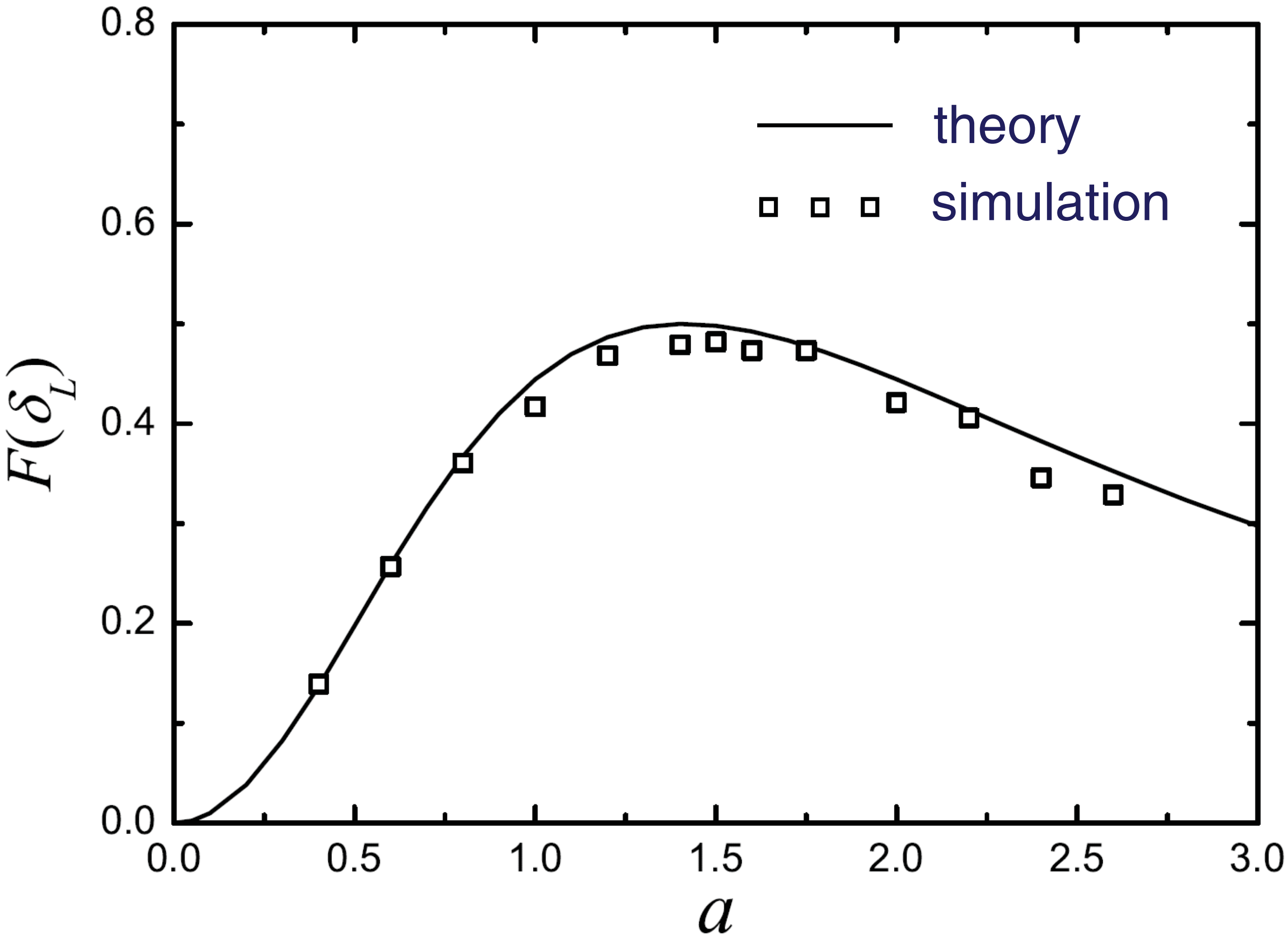

中央研究院

國立中央大學
National Central University

Joint Laboratory of High-Field Physics and Ultrafast Technology

Thank you for your attention!